



Rensselaer

**CERTS Project
Voltage Stability Applications using Synchrophasor Data**

**Report 11
Final Report**

Submitted by

**Joe H. Chow, Scott G. Ghiocel, Maximilian Liehr,
and Felipe Wilches-Bernal**

**Rensselaer Polytechnic Institute
110 8th Street
Troy, NY 12180-3590**

June 1, 2015

Prepared for

Dejan Sobajic, Project Manager

**Office of Electricity Delivery and Energy Reliability Transmission
Reliability Program of the U.S. Department of Energy Under Contract
No. DE-AC02-05CH11231**

Acknowledgement

The work described in this paper was coordinated by the Consortium for Electric Reliability Technology Solutions, and funded by the Office of Electricity Delivery and Energy Reliability, Transmission Reliability Program of the U.S. Department of Energy through a contract with Rensselaer Polytechnic Institute administered by the Lawrence Berkeley National Laboratory. This work was supported by the Lawrence Berkeley National Lab (LBL) subcontract 7040520 of prime contract DE-AC02-05CH11231 between LBL and Department of Energy (DOE). The authors gratefully acknowledge the support provided by Lawrence Berkeley National Lab (LBL) and Department of Energy (DOE).

Disclaimer

This document was prepared as an account of work sponsored by the United States Government. While this document is believed to contain correct information, neither the United States Government nor any agency thereof, nor The Regents of the University of California, nor any of their employees, makes any warranty, express or implied, or assumes any legal responsibility for the accuracy, completeness, or usefulness of any information, apparatus, product, or process disclosed, or represents that its use would not infringe privately owned rights. Reference herein to any specific commercial product, process, or service by its trade name, trademark, manufacturer, or otherwise, does not necessarily constitute or imply its endorsement, recommendation, or favoring by the United States Government or any agency thereof, or The Regents of the University of California. The views and opinions of authors expressed herein do not necessarily state or reflect those of the United States Government or any agency thereof, or The Regents of the University of California.

Table of Contents		page
Chapter 1	Introduction and Survey of Voltage Stability Methods	4
Chapter 2	AQ-Bus Method	10
Chapter 3	Thevenin Equivalent Calculation	11
Chapter 4	BPA Wind Hub Voltage Stability Analysis	12
Chapter 5	SCE Monolith Region Voltage Stability Analysis	24
Chapter 6	Technology Commercialization	30
Chapter 7	Conclusions and Recommendations	31

The radial power system is modeled by an equivalent Thevenin impedance $|Z_{\text{Thev}}|$ connected to an equivalent voltage source with a fixed voltage $|V_{\text{Thev}}|$. The main idea of this approach is that the load bus voltage is at the critical value when the load impedance $|Z_{\text{agg}}|$ is equal to the Thevenin impedance $|Z_{\text{Thev}}|$. This is also equal to the maximum power transfer P_{max} . Suppose that the current power transfer is P . Then the voltage-stability margin is $(P_{\text{max}} - P)$. If contingencies are considered, then P_{max} is the maximum power transfer under the worst contingency.

In this technique, beside the radial system requirement, it is important that $|V_{\text{Thev}}|$ and $|Z_{\text{Thev}}|$ are computed properly. This computation can be achieved by using system data or measured data. Analytically, one only needs two sufficiently different sets of load voltage and current to compute the Thevenin voltage and impedance. If more data is available, such as in the case of a PMU continuously monitoring the power system data, a least-squares approach for computing and real-time updating the Thevenin equivalent can be taken. In fact, ABB has a product that supports this approach [1.6].

An enhancement to the Thevenin equivalent model is to include the impact of the voltage regulator, of which a schematic is shown in Figure 1.2(b). A discussion of such dynamic models can be found in [1.5].

1.3 Voltage Stability Analysis of Large Systems

In a large power system, voltage stability is determined by increasing the active and reactive power load until the critical voltage value is reached. Unfortunately the Newton-Raphson loadflow algorithm would diverge because the loadflow Jacobian matrix will become singular at the critical voltage value. This singularity can be measured by the gap between the largest and smallest singular value of the Jacobian matrix. To amend the ill-conditioning situation, the method of homotopy has been proposed [1.7,1.8]. In a homotopy method, a parameter λ is introduced and the method of derivative is used to continue the solution. At $\lambda = 0$, one has the initial problem which is readily solved. When $\lambda = 1$ or some other positive value, one obtains the solution to the difficult to solve problem.

When used for voltage stability analysis, given a number of interconnected PQ and PV buses, a loadflow formulation is given by the nonlinear equation

$$f(V, \theta, P, Q) = 0 \quad (1.1)$$

where V is the bus voltage magnitude, θ is the bus voltage angle, and P and Q are the bus active power and reactive power, respectively, of generators and loads. In the continuation method, a parameter λ is introduced to represent the increase in active and reactive power at certain load buses. As a result, the new loadflow equation can be formulation as

$$\bar{f}(V, \theta, P, Q, \lambda) = 0 \quad (1.2)$$

The solution of (1.2) for each new (increased) value of λ is obtained in two steps: first, a predictor step is to take the variables to be close to the new solution, and second, a corrector step is used to solve for the solution. This process is illustrated in Figure 1.3 by locating the loadflow solution on a PV curve. For example, at Point 1, the slope of the PV curve is computed and used to advance the system variables to be close to Point 2. This is the predictor step. Then the corrector step is used to

iteratively obtain the solution at Point 2. The process would continue until the voltage collapse point is reached.

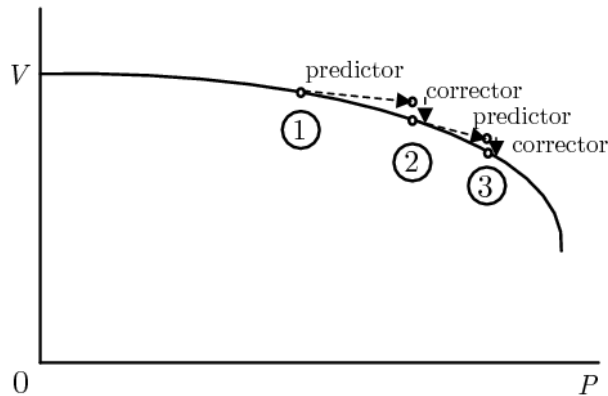


Figure 1.3: Predictor and corrector in the continuation power flow method

The CPFLOW program [1.9] demonstrated the application of the continuation method to large power systems, including a 3493-bus system. Currently, the continuation method is available in the Voltage Stability Assessment (VSA) program from Bigwood System, Inc., the IPFLOW program from EPRI (VSTAB), and the VSA program from Power Tech [1.10]. It should be noted that the Power Tech approach is based on an eigenvalue analysis of the loadflow Jacobian [1.10].

The ability to compute the critical voltage value and maximum power transfer level in a non-radial power system is important to the success of this project. The continuation method is one mechanism to circumvent the Jacobian singularity. Other mechanisms to more directly circumvent the Jacobian singularity condition will be explored.

1.4 Hybrid Voltage Stability Analysis Approach

For performing real-time voltage stability analysis of a regional load center, the VIP approach may not be applicable and the full-model analysis with the continuation power flow technique may require excessive computational resources. Thus there is an incentive to obtain a smaller power system relevant to the power stability analysis of a specific regional load center.

As an illustration, consider the Pacific AC Intertie shown in Figure 1.4. It is one of the power transfer paths into the Los Angeles area. There are also power transfer paths coming into LA from the east (Nevada and Arizona). Thus the voltage stability analysis of the LA area requires a model with several inflow paths. However, the VS analysis of the LA area clearly does not warrant using the complete WECC model. The hybrid approach is to develop a reduced model, possibly with multiple power in-feeds, that would be suitable for the voltage stability analysis of a regional load center. An impetus of the method is the availability of PMU data for model update and sensitivity models at the injection points.

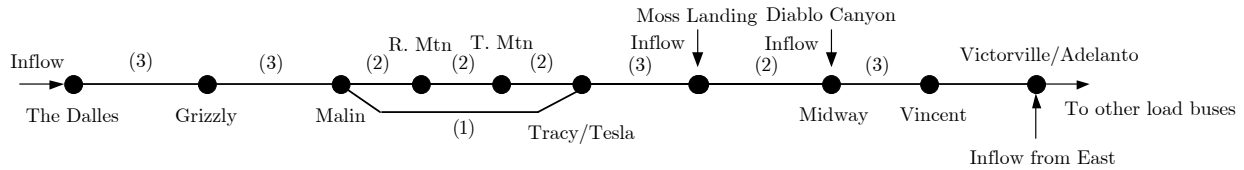


Figure 1.4: A simplified Pacific AC Intertie

There are some initial research activities in developing the hybrid model approach, notably the work of Dr. Kai Sun [1.11,1.12]. In this project, we will provide a systematic procedure to develop hybrid models for voltage stability analysis and investigate efficient methods for calculating voltage collapse points and hence voltage stability margins.

1.5 Use of PMU Data for Voltage Stability Analysis

If voltage and phasor measurements at a load bus are available, then the active and reactive power consumption of the load can be measured. Given a disturbance affecting the power transfer to the load center, one can readily obtain a plot of the power versus voltage curve, such as the plot shown in Figure 1.5, which can be treated as part of a PV curve [1.13]. A similar PV curve was obtained for the Southern California Edison System [1.14]. This technique has been adopted by EPG as a feature in its real-time phasor visualization program RTDMS.

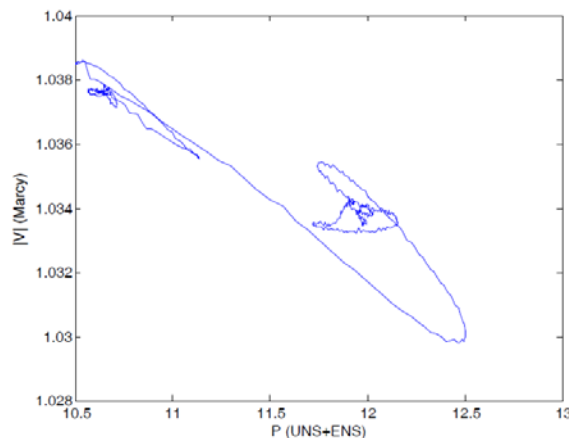


Figure 1.5: Dynamic PV curve at a Bus in Central New York

In using PMU data for voltage stability analysis, it is important that the measured phasor data are of high quality. For this purpose, we are developing a phasor state estimator to enhance the quality of the phasor data [1.15,1.16]. In this project, we will extend this technology to the hybrid VS analysis approach.

1.6 Voltage Stability Indices

For operation purposes, the outcome of a voltage stability analysis is typically an index or several indices, to allow for the development of some appropriate operator actions. The voltage stability indices include [1.5]:

1. Reactive power reserves – the amount of automatically activated reactive power reserve in effective locations.
2. Voltage drop – voltage drops as power transfer level increases.

3. MW/MVAR losses – power losses increase rapidly as a system approaches voltage collapse.
4. Incremental steady-state margin – an indicator based on the determinant of the power flow Jacobian.
5. Minimum singular value or eigenvalue – an index based on the closeness of the minimum singular value or eigenvalue of the power flow Jacobian to zero.

6. Approach of the Current Project

Guided by the literature review, in this project, we have made contributions to three areas.

1. A new AQ-bus method to compute the voltage stability margin, which can bypass the singularity condition of the power flow Jacobian matrix.
2. Voltage stability analysis of a small load area, with Thevenin equivalents representing the connections of the small load area to the bulk power system. This method is suitable for wind hub installation at median/low voltage transmission/distribution systems.
3. Applications of the method to a wind hub in the BPA transmission system, and a wind hub in the SCE transmission/distribution system.

These results will be discussed in the remainder of the report.

References

- [1.1] C. Launay, "Prevention of Voltage Collapse on the French Power System," *IEE Colloquium on International Practices in Reactive Power Control*, pp. 2/1-2/7, 1993.
- [1.2] A. Kurita and T. Sakurai, "The Power System Failure on July 23, 1987 in Tokyo," *Proc. 27th IEEE Conf on Decision and Control*, pp. 2093-2097, 1988.
- [1.3] C. Taylor, *Power system voltage stability*, McGraw Hill, 1994.
- [1.4] T. Van Cutsem and C. Vournas, *Voltage stability of electric power systems*, Kluwer Academic Publishers, 1998.
- [1.5] V. Ajjarapu, *Computational techniques for voltage stability assessment and control*, Springer, 2006.
- [1.6] D. E. Julian, R. P. Schulz, K. T. Vu, W. H. Quaintance, N. B. Bhatt, and D. Novosel, "Quantifying Proximity to Voltage Collapse using the Voltage Instability Predictor (VIP)," *Proc. IEEE PES Summer Power Meeting*, July 2000, vol. 2, pp. 931-936.
- [1.7] K. Iba, H. Suzuki, M. Egawa, and T. Watanabe, "Calculation of Critical Loading Condition with Nose Curve using Homotopy Continuation Method," *IEEE Transactions on Power Systems*, vol. 6, pp. 584-593, 1991.
- [1.8] V. Ajjarapu and C. Christy, "The Continuation Power Flow: A Tool to Study Steady State Voltage Stability," *IEEE Transactions on Power Systems*, vol. 7, pp. 416-423, 1992.
- [1.9] H.-D. Chiang, A. J. Fluech, K. S. Shah, and N. Balu, "CPFLOW: A Practical Tool for Tracing Power System Steady-State Stationary Behavior Due to Load and Generation Variations," *IEEE Transactions on Power Systems*, vol. 10, pp. 623-634, 1995.
- [1.10] P. Kundur, *Power system dynamics and control*, McGraw Hill, 1994.
- [1.11] K. Sun, P. Zhang, and L. Min, "Measurement-based Voltage Stability Monitoring and Control for Load Centers," EPRI Technical Report PID#1017798, 2009.
- [1.12] E. Farantatos, K. Sun, and A. Del Rosso, "A Hybrid Framework for Voltage Security Assessment Integrating Simulation- and Measurement-Based Approaches," EPRI Technical Report PID#1024260, 2012.

- [1.13] S. G. Ghiocel, J. H. Chow, X. Jiang, G. Stefopoulos, B. Fardanesh, D. B. Bertagnolli, and M. Swider, "A voltage sensitivity study on a power transfer path using synchrophasor data," *Proceedings of IEEE PES GM, Detroit, MI*, July 2011.
- [1.14] M. Parniani, J. H. Chow, L. Vanfretti, B. Bhargava, and A. Salazar, "Voltage stability analysis of a multiple-infeed load center using Phasor Measurement Data," *Proc. 2006 IEEE Power System Conference and Exposition*.
- [1.15] L. Vanfretti, J. H. Chow, A. Sarawgi, and B. Fardanesh, "A phasor-data-based state estimator incorporating phase bias correction," *IEEE Transactions on Power Systems*, vol. 26, pp. 111-119, 2011.
- [1.16] S. G. Ghiocel, J. H. Chow, G. Stefopoulos, B. Fardanesh, D. Maragal, D. B. Bertagnolli, M. Swider, M. Razanousky, D. J. Sobajic, and J. H. Eto, "Phasor-Measurement-Based Voltage Stability Margin Calculation for a Power Transfer Interface with Multiple Injections and Transfer Paths," *Proceedings of Power System Computation Conference, Wroclaw, Poland*, 2014.

Chapter 2: AQ-Bus Method

The details of the AQ-bus method are contained in the paper

S. G. Ghiocel and J. H. Chow, "A Power Flow Method using a New Bus Type for Computing Steady-State Voltage Stability Margins," *IEEE Transactions on Power Systems*, vol. 29, no. 2, pp. 958-965, 2014.

The paper is attached below.

A Power Flow Method using a New Bus Type for Computing Steady-State Voltage Stability Margins

Scott G. Ghiocel, *Student Member, IEEE* and Joe H. Chow, *Fellow, IEEE*

Abstract—In steady-state voltage stability analysis, it is well-known that as the load is increased toward the maximum loading condition, the conventional Newton-Raphson power flow Jacobian matrix becomes increasingly ill-conditioned. As a result, the power flow fails to converge before reaching the maximum loading condition. To circumvent this singularity problem, continuation power flow methods have been developed. In these methods, the size of the Jacobian matrix is increased by one, and the Jacobian matrix becomes non-singular with a suitable choice of the continuation parameter.

In this paper, we propose a new method to directly eliminate the singularity by reformulating the power flow. The central idea is to introduce an AQ bus in which the bus angle and the reactive power consumption of a load bus are specified. For steady-state voltage stability analysis, the voltage angle at the load bus can be varied to control power transfer to the load, rather than specifying the load power itself. For an AQ bus, the power flow formulation consists of only the reactive power equation, thus reducing the size of the Jacobian matrix by one. This reduced Jacobian matrix is nonsingular at the critical voltage point. We illustrate the method and its application to steady-state voltage stability using two example systems.

Index Terms—Voltage stability analysis, voltage stability margin, Jacobian singularity, angle parametrization, AQ bus

I. INTRODUCTION

Voltage instability has been the cause of many major blackouts [1, 2, 3]. In a power system operation environment, it is important to ensure that the current operating condition is voltage stable subject to all credible contingencies. Methods for calculating the stability margin for each contingency can be classified into two categories: dynamic (time-domain simulation) and steady-state (power flow methods) [4, 5]. Time-domain simulation can capture the dynamic elements of voltage instability. In this paper we are only dealing with steady-state voltage stability analysis occurring over a long time span.

One difficulty in steady-state voltage stability analysis is that the conventional Newton-Raphson power flow fails to converge as the maximum loadability point is reached. In the unconstrained case, the Jacobian matrix J becomes singular at maximum loading, and the power flow solution will not converge when the smallest singular value of J becomes too small [4, 5].

To circumvent this singularity problem, continuation power flow methods based on homotopy techniques have been developed [6, 7]. In this approach, a load-increase continuation parameter λ is introduced as an additional variable. As a

Table I
POWER FLOW BUS TYPES

Bus types	Bus representation	Fixed values
PV	Generator buses	Active power generation and bus voltage magnitude
PQ	Load buses	Active and reactive consumption
AV	Swing bus	Voltage magnitude and angle
AQ	Load buses	Voltage angle and reactive power consumption

result, the size of the Jacobian matrix is increased by one, which becomes non-singular with a suitable choice of the continuation parameter. The continuation power flow is solved in a two-step process with a predictor step and a corrector step, and requires additional manipulations and computation [8]. During the corrector step, the continuation method still needs to deal with a poorly conditioned Jacobian.

In this paper, we propose a new power flow method to directly eliminate the singularity issue without adding the additional complexity required by such homotopy methods. Elimination of the singularity allows for a well-conditioned power flow solution even at the maximum loadability point. The central idea is to reformulate the power flow with the introduction of a new type of load bus, which we call an AQ bus (A stands for angle). A conventional power flow formulation uses three types of buses: PV buses, PQ buses, and the swing bus (Table I¹). For an AQ bus, the bus voltage angle θ and the reactive power consumption Q are specified. In this sense, a swing bus can be considered as an AV bus, because its angle is fixed and its voltage magnitude is known. In this formulation, the active power balance equation at the AQ load bus is no longer needed. Only the reactive power balance equation is kept. Furthermore, because θ at this bus is known, it is eliminated from the power flow solution vector consisting of bus voltage magnitudes of PQ buses and bus voltage angles of all the buses except for the swing bus. Thus the size of the resulting Jacobian matrix J_R is reduced by one. This J_R matrix is nonsingular at the maximum loadability point, and thus it avoids the singularity problem of the conventional Jacobian matrix J .

The load increase on Bus B_L , when specified as an AQ bus in this new power flow method, is achieved by increasing the bus voltage angle separation θ_s between Bus B_L and the swing bus. It is expected that the load P_L will increase with θ_s until

S. Ghiocel and J. Chow are with the Department of Electrical, Computer, and Systems Engineering, Rensselaer Polytechnic Institute, Troy, NY 12180, USA. (e-mail: ghiocel@alum.rpi.edu, chowj@rpi.edu)

¹A recent paper [9] lists 16 bus types, of which the AQ or θQ bus is one of them. The paper addresses only the solvability issue of the Bus-type Extended Load Flow (BELF), without addressing specifically the voltage stability margin calculation using the AQ -bus formulation.

the critical voltage point, then further increases in θ_s will result in a decrease of P_L . For each value of θ_s , the amount of P_L is not known until the power flow is solved. This eliminates the active power balance equation at the load bus B_L . The reactive power balance equation at B_L is still maintained. For load increases involving constant-power-factor loads and at multiple buses, additional expressions are needed to develop the reduced Jacobian matrix J_R . The computation of voltage stability margins using this method is no more complicated than a conventional load flow solution and the step size in increasing θ to reach the critical voltage point is not limited. In addition, computation-speed enhancement techniques such as decoupled power flow can still be used [10].

This paper is organized as follows. In Section II, we use a single-load stiff-bus model to motivate the new problem formulation. Sections III provides the general framework of the approach. Section IV uses two example test systems to illustrate the method.

II. MOTIVATION

Consider the two-bus power system shown in Fig. 1, in which the load bus is connected via a reactance X to the stiff voltage source with $E = 1$ pu and its angle set to zero. The load is denoted by a voltage of magnitude V_L and phase $-\theta_s$, and a power consumption $P_L + jQ_L$. The angle θ_s is positive so that power is transferred from the stiff source to the load. Following [4], we will consider the power flow solutions of the system for constant power load where $Q_L = P_L \tan(\phi)$, where $\cos(\phi)$ is the power factor (ϕ is positive for lagging and negative for leading).

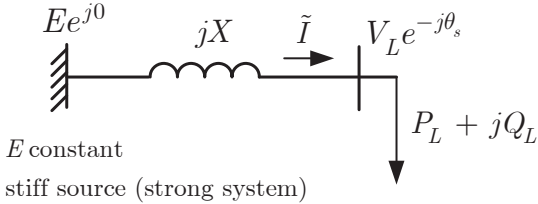


Figure 1. A two-bus power system

There are two relevant power flow equations for this system, both for the load bus:

$$P_L = -\frac{V_L E \sin \theta_s}{X}, \quad Q_L = \frac{V_L E \cos \theta_s}{X} - \frac{V_L^2}{X} \quad (1)$$

Treating the load bus as a PQ bus, the Jacobian matrix obtained by taking the partial derivatives of these two equations with respect to θ_s and V_L is

$$J = -\frac{1}{X} \begin{bmatrix} V_L E \cos \theta_s & E \sin \theta_s \\ V_L E \sin \theta_s & 2V_L - E \cos \theta_s \end{bmatrix} \quad (2)$$

The Jacobian J is singular when

$$\det J = (2V_L \cos \theta_s - E)/X = 0 \quad (3)$$

which occurs at the critical voltage point.

If the load bus is taken as an AQ bus, then the separation angle θ_s can be specified without specifying P_L and the active power equation is no longer needed. If Q_L is fixed, then the

reduced matrix J_R is simply the (2,2) entry of J (2). Here the load is of constant power factor, i.e., $Q_L = P_L \tan \phi$, allowing the reactive power equation to be rewritten as

$$Q_L = \frac{V_L E \cos \theta_s}{X} - \frac{V_L^2}{X} = -\frac{V_L E \sin \theta_s}{X} \tan \phi \quad (4)$$

that is,

$$0 = \frac{V_L E \cos \theta_s}{X} - \frac{V_L^2}{X} + \frac{V_L E \sin \theta_s}{X} \tan \phi \quad (5)$$

The reduced Jacobian is the partial derivative of (5) with respect to V_L

$$J_R = \frac{1}{X} (E \cos \theta_s - 2V_L + E \sin \theta_s \tan \phi) \quad (6)$$

which is singular when $J_R = 0$.

For the 2-bus system in Fig. 1, we explore the singularities of the Jacobians (2) and (6). Using $E = 1$ pu and $X = 0.1$ pu, we plot the variation of θ_s , P_L , V_L , and the determinants of J and J_R , for 0.9 lagging, unity, and 0.9 leading power factor loads. Fig. 2 shows the familiar PV curve. The singularity of J occurs when the slope of the PV curve becomes infinite.

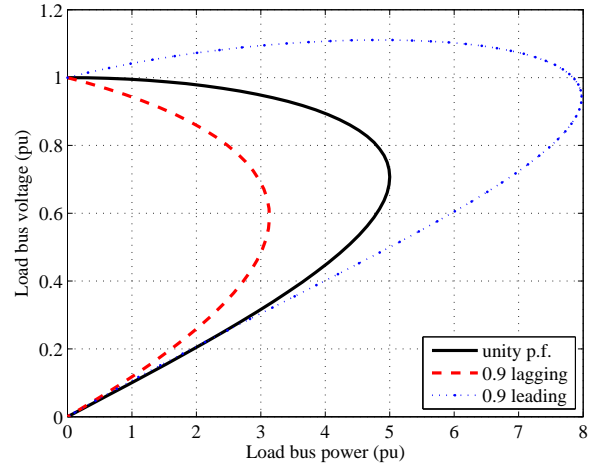
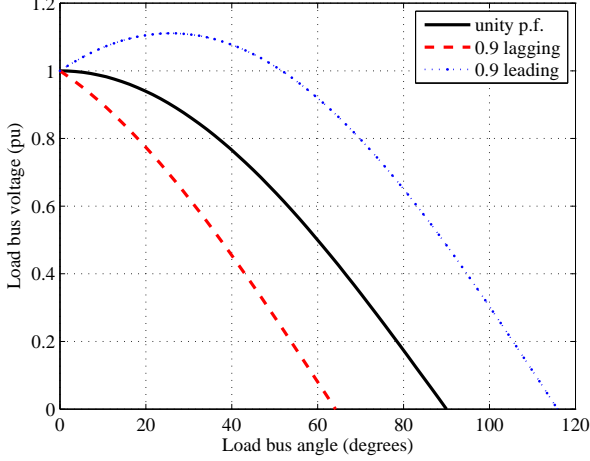
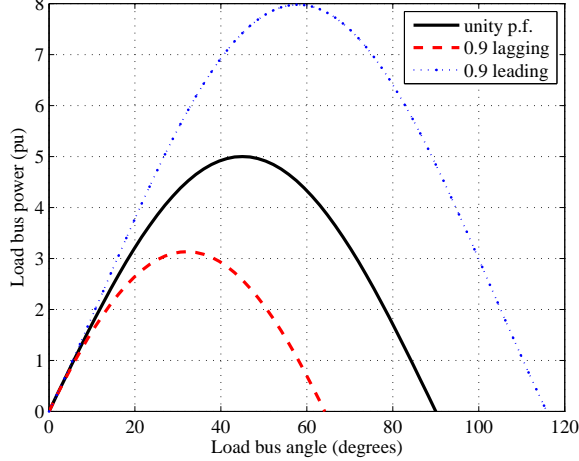
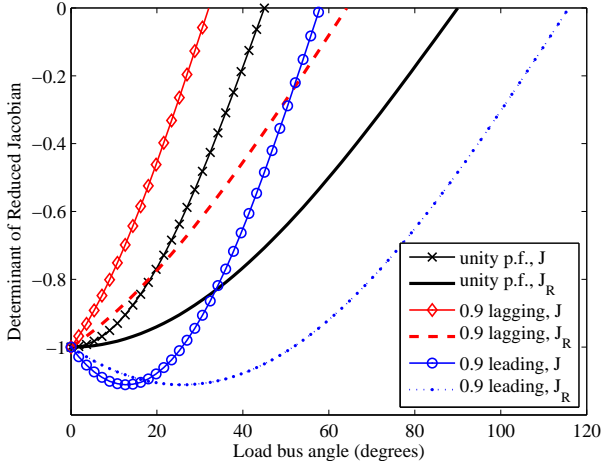


Figure 2. PV curves

Figs. 3 and 4 show the variation of V_L and P_L versus θ_s . The slopes of these curves are finite within the complete operational range of the angle separation. The peak of each P_L curve in Fig. 4 corresponds to the value of the separation angle θ_c at the critical voltage point. Note that the power factor of the load determines the maximum θ_s that is feasible.

The values of the determinants of J and J_R are shown in Fig. 5. It is obvious that $\det(J) = 0$ at θ_c , the value of the angle separation at the critical voltage point. On the other hand, J_R remains nonzero at θ_c , such that the Newton-Raphson iteration scheme will readily converge. In addition, $J_R = 0$ only when the load bus voltage V_L is zero.

Figs. 4 and 5 show that the separation angle θ_s is a useful variable to provide additional insights into the voltage stability problem. Most voltage stability analysis investigations have focused directly on V_L and largely ignored following up on θ_s .

Figure 3. Variation of V_L versus θ_s Figure 4. Variation of P_L versus θ_s Figure 5. Determinant of J and J_R as a function of θ_s

III. THEORETICAL FRAMEWORK AND COMPUTATION ALGORITHMS

In this section, we consider the general framework of a power flow formulation including an AQ bus, and extend the method for steady-state voltage stability analysis allowing for load and generation increases on multiple buses and for constant power factor loads.

Consider a power system with N_G generator buses and N_L load buses, such that the total number of buses is $N = N_G + N_L$. Let Bus 1 be the swing bus, Buses 2 to N_G be the generator PV buses, and Buses $N_G + 1$ to N be the load PQ buses.

The power flow problem consists of solving the active and reactive power injection balance equations

$$\Delta P_i = P_i - f_{P_i}(\theta, V) = 0, \quad i = 2, \dots, N \quad (7)$$

$$\Delta Q_i = Q_i - f_{Q_i}(\theta, V) = 0, \quad i = N_G + 1, \dots, N \quad (8)$$

where P_i and Q_i are the scheduled active and reactive power injections at Bus i . Vectors V and θ contain the bus voltage magnitudes and angles, and $f_{P_i}(\theta, V)$ and $f_{Q_i}(\theta, V)$ are the computed active and reactive power injections, respectively. ΔP is the vector of active power mismatches at Buses 2 to N , and ΔQ is the vector of reactive power mismatches at Buses $N_G + 1$ to N .

The power flow problem is commonly solved by the Newton-Raphson method, using the iteration

$$J \begin{bmatrix} \Delta \theta \\ \Delta V \end{bmatrix} = \begin{bmatrix} J_{11} & J_{12} \\ J_{21} & J_{22} \end{bmatrix} \begin{bmatrix} \Delta \theta \\ \Delta V \end{bmatrix} = \begin{bmatrix} \Delta P \\ \Delta Q \end{bmatrix} \quad (9)$$

where the Jacobian matrix J is a square matrix of dimension $(2N - N_G - 1)$ containing the partial derivatives of the active and reactive power flow equations with respect to the bus angles θ and the voltage magnitudes V , where

$$J_{11} = \frac{\partial f_P}{\partial \theta}, \quad J_{12} = \frac{\partial f_P}{\partial V}, \quad J_{21} = \frac{\partial f_Q}{\partial \theta}, \quad J_{22} = \frac{\partial f_Q}{\partial V} \quad (10)$$

$$\theta = [\theta_2 \quad \dots \quad \theta_N]^T \quad (11)$$

$$V = [V_{N_G+1} \quad \dots \quad V_N]^T \quad (12)$$

$\Delta \theta$ and ΔV are the corrections on θ and V , respectively.

A. Power flow formulation including an AQ bus

Suppose Bus N is an AQ bus with $\theta_N = \theta_N^\circ$ and Q_N specified, then the Newton-Raphson iteration reduces to

$$J_R \begin{bmatrix} \Delta \theta_R \\ \Delta V \end{bmatrix} = \begin{bmatrix} J_{R11} & J_{R12} \\ J_{R21} & J_{R22} \end{bmatrix} \begin{bmatrix} \Delta \theta_R \\ \Delta V \end{bmatrix} = \begin{bmatrix} \Delta P_R \\ \Delta Q \end{bmatrix} \quad (13)$$

where

$$J_{R11} = J_{11}(1 \dots N-2; 1 \dots N-2)|_{\theta_N=\theta_N^\circ} \quad (14)$$

$$J_{R12} = J_{12}(1 \dots N-2; 1 \dots N-N_G)|_{\theta_N=\theta_N^\circ} \quad (15)$$

$$J_{R21} = J_{21}(1 \dots N-N_G; 1 \dots N-2)|_{\theta_N=\theta_N^\circ} \quad (16)$$

$$J_{R22} = J_{22}|_{\theta_N=\theta_N^\circ} \quad (17)$$

The number of bus angle variables is reduced by one, such that

$$\Delta \theta_R = [\Delta \theta_2 \quad \dots \quad \Delta \theta_{N-1}]^T \quad (18)$$

The AQ bus active power flow equation is eliminated, such that ΔP_R is the vector of active power mismatches at Buses 2 to $(N-1)$. The load P_N on Bus N is no longer specified, but it can be computed using $f_{P_i}(\theta, V)$.

This reduced power flow formulation would not yield directly a specific P_N on Bus N . However, this is not a hindrance in voltage stability analysis. Instead of increasing P_N on Bus N and not knowing whether the non-convergent result is actually the maximum loadability point, a user can keep increasing the angular separation between Bus N and the swing bus until the maximum power transfer point is reached. The reduced Jacobian J_R would not be singular at that point and the maximum loadability point can be readily computed.

B. Voltage stability analysis for constant-power-factor loads

In voltage stability analysis, it is common to specify constant-power-factor loads. In this section, we will extend the iteration (13) to a more general case by considering constant-power-factor load increases at multiple load buses to be supplied by generators at multiple locations.

Let Buses N_p to N be load buses with constant power factor $\cos \phi_\ell$, that is, $Q_\ell = P_\ell \tan \phi_\ell$ for $\ell = N_p, \dots, N$. The active power load increases at these load buses are scaled with respect to Bus N , that is,

$$P_\ell - P_\ell^0 = \alpha_\ell (P_N - P_N^0), \quad \ell = N_p, \dots, N-1 \quad (19)$$

The load increase is balanced by increases in outputs of generators on Buses 1 to q , with the active power at these generators scaled according to the swing bus

$$P_k - P_k^0 = \beta_k (P_1 - P_1^0), \quad k = 2, \dots, q \quad (20)$$

In a solved power flow solution, the active power injections at Buses 1 and N are computed as the power flow leaving the buses on the lines interconnecting them to the other buses. Thus in an AQ -bus formulation, we account for the groups of increasing load and generation by modifying the power flow injection equations such that

$$f_{P_k}(V, \theta) = \beta_k f_{P_1}(V, \theta), \quad k = 2, \dots, q \quad (21)$$

$$f_{P_\ell}(V, \theta) = \alpha_\ell f_{P_N}(V, \theta), \quad \ell = N_p, \dots, N-1 \quad (22)$$

$$f_{Q_\ell}(V, \theta) = \alpha_\ell f_{P_N}(V, \theta) \tan \phi_\ell, \quad \ell = N_p, \dots, N-1 \quad (23)$$

The other injection equations remain unchanged.

In obtaining a new reduced Jacobian matrix to solve this new power flow problem, we need two row vectors of partial derivatives of f_{P_1} and f_{P_N}

$$J_i = \left[\frac{\partial f_{P_1}}{\partial \theta_R}, \quad \frac{\partial f_{P_1}}{\partial V} \right], \quad i = 1, N \quad (24)$$

where J_i is the i th row of the Jacobian. Note that J_N is row $N-1$ of J without the entry due to $\Delta \theta_N$, and J_1 is not contained in J because Bus 1 is the swing bus.

Thus the reduced Jacobian J_R in (13) for the fixed reactive power injection problem is modified to form a new reduced

Jacobian \bar{J}_R , such that

$$\bar{J}_{Ri} = J_{Ri} - \beta_k J_1, \quad i = 1, \dots, q-1, \quad k = 2, \dots, q \quad (25)$$

$$\bar{J}_{Ri} = J_{Ri} - \alpha_\ell J_N, \quad i = N_p - 1, \dots, N-2, \\ \ell = N_p, \dots, N-1 \quad (26)$$

$$\bar{J}_{Ri} = J_{Ri} - \alpha_\ell J_N \tan \phi_\ell, \quad i = N_{J_R} - N_p, \dots, N_{J_R}, \\ \ell = N_p, \dots, N-1 \quad (27)$$

where $N_{J_R} = 2N - N_G - 2$ is the dimension of J_R . The other rows of J_R remain unchanged.

In this more general formulation of the AQ -bus power flow, the Newton-Raphson iteration becomes

$$\bar{J}_R \begin{bmatrix} \Delta \theta_R \\ \Delta V \end{bmatrix} = \begin{bmatrix} \Delta P_R \\ \Delta Q \end{bmatrix} \quad (28)$$

where the power mismatch (21)-(23) is based on the previous iteration. In voltage stability margin calculations, the injection solution at a lower angle separation condition can be used to initiate the solution process.

C. Algorithms for computing voltage stability margins

Because \bar{J}_R in (28) would not be singular at the maximum loadability point, fast and well-conditioned voltage stability margin calculation methods can be formulated. Here we present two algorithms for steady-state voltage stability analysis as basic applications of the AQ -bus method.

Algorithm 1: using AQ -bus power flow with \bar{J}_R to compute voltage stability margins

- 1) From the current operating point (base case) with a power transfer of P_0 , specify the load and generation increment schedule, and the load composition (such as constant power factors).
- 2) Use a conventional power flow program with increasing loads until the Newton-Raphson algorithm no longer converges.
- 3) Starting from the last converged solution in Step 2, apply the AQ -bus power flow method (19)-(28) to continue the power flow solution by increasing the angle separation ($\theta_1 - \theta_N$) between the AQ bus and the swing bus until the maximum power transfer $P_{0\max}$ is reached. Typically, the bus with the largest load increase will be selected to be the AQ bus. The base-case voltage stability margin is $P_{0m} = P_{0\max} - P_0$.
- 4) Specify a set of N_c contingencies to be analyzed.
- 5) For contingency i , repeat Steps 2 and 3 for the post-contingency system to compute the maximum power transfer $P_{i\max}$ and the voltage stability margin $P_{im} = P_{i\max} - P_0$.
- 6) Repeat Step 5 for all contingencies $i = 1, 2, \dots, N_c$.
- 7) The contingency-based voltage stability margin, measured as additional power delivered to the load until the maximum loadability point, is given by

$$P_m = \min_{i=0, \dots, N_c} \{P_{i\max}\} \quad (29)$$

Note that for any of the contingencies in Step 5, if the AQ -bus algorithm for P_0 fails to converge, that is, P_0 is not a

feasible solution, then the AQ -bus algorithm can be used to reduce P_0 until a converged power flow solution is obtained. The new power flow solution would then be a voltage secure operating condition.

Also note in Steps 3 and 5 of Algorithm 1, all the capability of the conventional power flow can be used. For example, taps can be adjusted to maintain voltages, and generators exceeding their reactive power capability can be changed to PQ buses from PV buses. Both capabilities are important for finding the proper voltage stability limit.²

The advantage of using a conventional power flow algorithm in Step 2 of Algorithm 1 is that it will allow a user to select the AQ bus for Step 3. There are several ways to select the AQ bus: (1) use the bus with the largest load increase (as stated in Step 3 of Algorithm 1), (2) use the bus with the largest rate of decrease of the bus voltage magnitude, or (3) use the bus angle with the largest component in the singular vector of the smallest singular value of J from the last converged solution. Frequently all three will yield the same bus.

It is also possible to solve for voltage stability margins without updating J_R (13). This method can be useful when one wants to avoid changing or reprogramming the Jacobian matrix entries, but it has slower convergence. The load increase condition (19), the generator increase condition (20), and the load power factor condition $Q_\ell = P_\ell \tan \phi_\ell$ are now enforced as fixed values after each power flow iteration has converged.

To be more specific, start from the nominal power flow solution with the load on Bus N at P_0 . The angular separation of Bus N and the swing bus is increased without changing any injections. The power flow is solved, and the resulting load at Bus N and the generation at the swing bus are computed. This new value P_N is used to compute the load increase on the other load buses (19), to be balanced by the generations according to (20). These new load and generation values are used to solve for another AQ -bus power flow. The process is repeated until the load and generation proportions are within tolerance. This procedure is summarized in the following algorithm.

Algorithm 2: using unmodified J_R to compute voltage stability margins

- 1) From the current operating point (base case) with a power transfer of P_0 , determine the load and generation increment schedule, and the load composition (such as constant power factor).
- 2) Use a conventional power flow program with increasing loads until the Newton-Raphson algorithm no longer converges.
- 3) Starting from the last converged solution in Step 2, apply the AQ -bus power flow algorithm (13) by increasing the angle separation between the AQ bus and the swing bus, to obtain a converged value of load at Bus N as P_N .
- 4) Update the loads and generations at the other buses according to (19) and (20), respectively, and repeat the power flow solution, until (19) and (20) are satisfied.

²Chapter 3 of [7] contains a more detailed discussion of voltage stability margin calculation for equipment reaching their reactive power output limits. At the breaking point, the smallest singular value of the conventional Jacobian matrix may not be exactly zero. The AQ -bus method can still be useful if the regular power flow cannot converge at the breaking point.

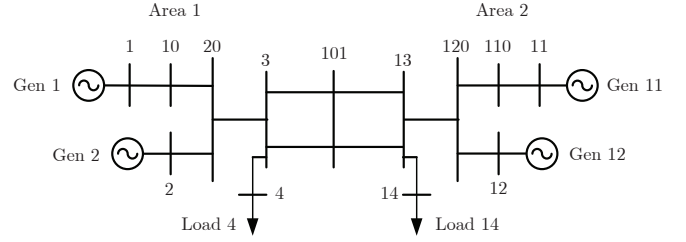


Figure 6. Two-area, four-machine power system

- 5) Increase the angular separation between Bus N and the swing bus and repeat Steps 3 and 4 until the load power at Bus N reaches the maximum value.
- 6) Apply Steps 4 to 7 of Algorithm 1 using Steps 2 to 5 of this algorithm to find the contingency-based voltage stability margin.

It is expected that Algorithm 2 would be slower than Algorithm 1. However, in Algorithm 2, minimal additional code for the Jacobian is needed.

IV. ILLUSTRATIVE EXAMPLES

In this section the AQ -bus power flow approach is applied to solve for the voltage stability margin of a 2-area, 4-machine system, and a 48-machine system.

A. Two-area system

We first use the Klein-Rogers-Kundur 2-area, 4-machine system [11] shown in Fig. 6 to illustrate the method. In this system, Load 14 will be increased at a constant power factor of 0.9 lagging whereas Load 4 is kept constant at $9.76 + j1$ p.u. The load increase is supplied by Generator 1. It is assumed that all the generators have unlimited reactive power supply.

Using Algorithm 1, the conventional power flow solution is shown as the black dashed line of the PV curve in Fig. 7. It fails to converge when the active power of Load 14 is $P_{14} = 19.15$ pu which occurs when the angle separation is $\theta_1 - \theta_{14} = 91.1^\circ$. After this point, the AQ -bus approach is used to continue the power flow solution by further increasing the angle separation between Buses 1 and 14. The solution of the AQ -bus approach is shown as the solid line of the PV curve in Fig. 7. From the PV curve, the critical voltage is 0.8144 p.u. and the maximum active load power is 19.2 p.u., with a power factor of 0.9 lagging.

We also plot the load active power at Bus 14 versus the angle separation $\theta_1 - \theta_{14}$ with the black curves in Fig. 8. Note that at maximum power transfer, $\theta_1 - \theta_{14} = 99.5^\circ$.

1) *Singular value analysis:* At the maximum loadability point, the largest singular value of J is 423 and the two smallest singular values are 3.59 and 0.02. At the same operating point, the largest and smallest singular values of the \bar{J}_R matrix are 423 and 2.49, respectively. Thus \bar{J}_R does not exhibit any singularity or convergence problems.

At the point where the conventional power flow fails to converge, the smallest singular value of the Jacobian is 0.05 and its singular vector is given in Table II. Note that the element of the singular vector with the largest magnitude corresponds to θ_{14} , the bus angle of the chosen AQ bus.

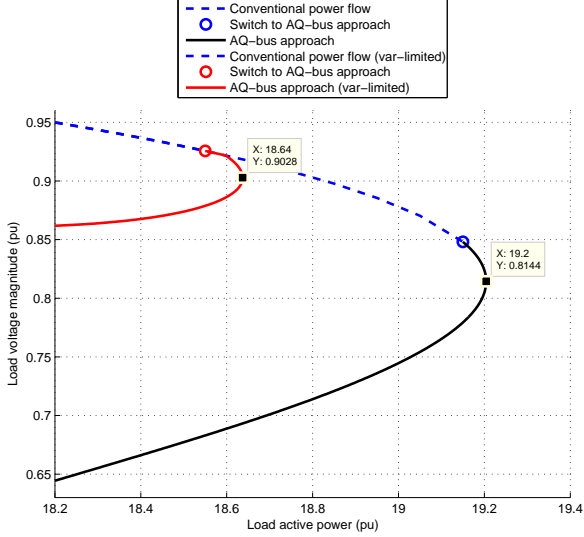


Figure 7. Power-voltage (PV) curves of two-area system, computed using Algorithm 1

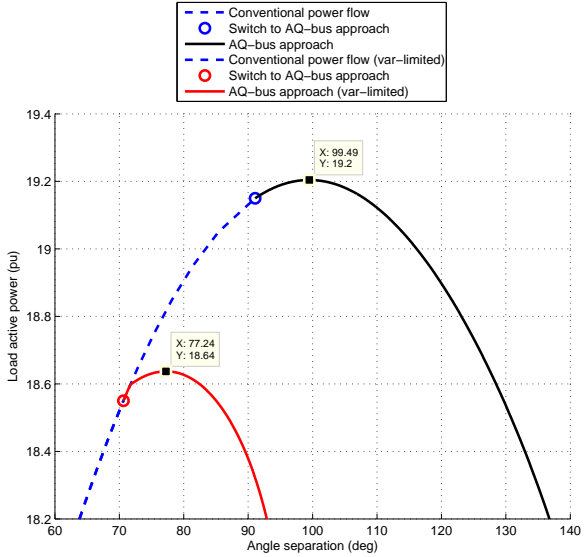


Figure 8. Power-angle ($P\theta$) curves of two-area system, computed using Algorithm 1

2) *Including var limits on a generator:* Because the AQ -bus power flow incorporates all the functionalities of a conventional power flow, we can readily demonstrate the effect of a var limit on a generator. Suppose we impose a maximum reactive power generation of 3 pu for Generator 2, that is, if the reactive power generation of Generator 2 exceeds 3 pu, it will be changed into a PQ bus with $Q = 3$ pu. The resulting PV and $P\theta$ curves for the same load increase conditions are shown as the red curves in Figs. 7 and 8.

Also of interest is the amount of reactive power provided by the four generators. Fig. 9 shows the reactive power plotted versus $\theta_1 - \theta_{14}$ for the var-limited case. We observe that the var limit on Generator 2 increases the reactive power burden on

Table II
SINGULAR VECTOR CORRESPONDING TO THE SMALLEST SINGULAR VALUE OF THE CONVENTIONAL POWER FLOW JACOBIAN

Singular vector component	Corresponding variable
0.025	θ_2
0.064	θ_3
0.075	θ_4
0.005	θ_{10}
0.329	θ_{11}
0.358	θ_{12}
0.416	θ_{13}
0.450	θ_{14}
0.031	θ_{20}
0.228	θ_{101}
0.332	θ_{110}
0.366	θ_{120}
0.085	V_3
0.086	V_4
0.021	V_{10}
0.117	V_{13}
0.125	V_{14}
0.048	V_{20}
0.172	V_{101}
0.024	V_{110}
0.062	V_{120}

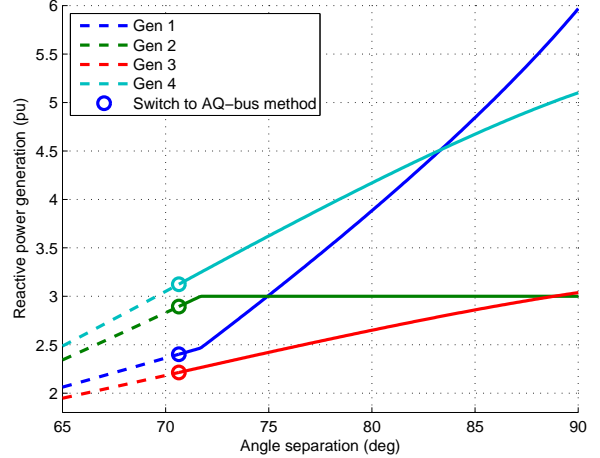


Figure 9. Reactive power output of generators in two-area system with a var limit

Generator 1, and the reactive power losses continue to increase after the point of maximum power transfer point, even though the active power consumed by the load decreases.

3) *Solution using Algorithm 2:* We applied Algorithm 2 to the two-area system and obtained the same results as with Algorithm 1. Note that with Algorithm 2, J_R is not modified to include the load and generator increase schedules. Thus Algorithm 2 is similar to a dishonest Newton method and needs more iterations than Algorithm 1.

B. NPCC 48-machine system

In this section we extend the AQ -bus power flow to a 48-machine NPCC (Northeast Power Coordinating Council) system [12] using Algorithm 1. A portion of the system map is given in Figure 10. For this system, we increase the loads on

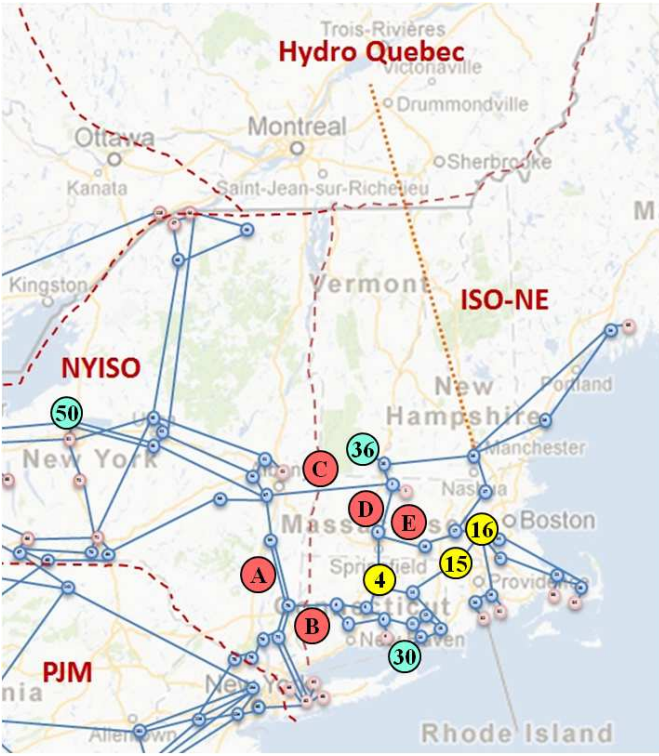


Figure 10. Map of the NPCC 48-machine system

Buses 4, 15, and 16 near Boston, with increased supply coming from the generators on Buses 30 and 36 in New England, and the generator on Bus 50 in New York, as indicated in Fig. 10. We choose Bus 50 as the swing bus and Bus 16 as the AQ bus. Generators on Buses 30 and 36 supply additional power as linear functions of the swing bus power output, as shown in Table III. Similarly, the loads on Buses 4 and 15 are scaled with respect to the AQ bus, as shown in Table IV.³ The loads at Buses 4, 15, and 16 all have a constant power factor of 0.95 lagging. All the other loads remain constant at their base values, and the active power generation for the other generators also remain constant.

Table III
GENERATOR SCHEDULE FOR 48-MACHINE SYSTEM

Generator Bus #	Bus Type	β_k
50	AV (swing)	-
30	PV	0.10
36	PV	0.80

Table IV
LOAD SCHEDULE FOR 48-MACHINE SYSTEM

Load Bus #	Bus Type	α_ℓ
16	AQ	-
4	PQ	0.50
15	PQ	0.25

We use the AQ-bus method to compute the PV curve for the base case, which is shown in Fig. 11 as the base case.

³Any of the buses in the load increase group (Buses 4, 15, and 16) can be chosen as the AQ bus for our method to work.

The method readily computes the PV curve to the maximum loadability point and beyond. The algorithm fails to converge when the system voltage is too low, because some load buses can no longer receive enough reactive power.

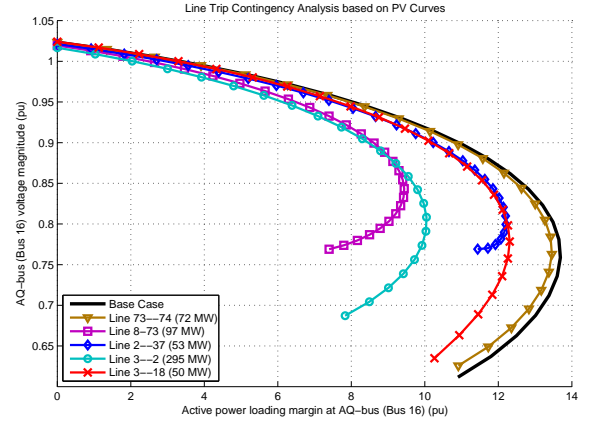


Figure 11. PV-curves for multiple contingencies on the NPCC 48-machine system

To demonstrate the computation of the voltage stability margin for contingency analysis, a set of line outage contingencies (A-E) is selected, as listed in Table V. The location of these lines are labeled in Fig. 10. In Fig. 11, we plot the computed PV curves for the five contingencies against the base case PV curve. Note that each power flow solution is designated with a plot marker in Fig. 11, demonstrating that the AQ-bus method does not require a small step size near the maximum power transfer point. In this example we used a step size of 5° but larger angle steps can be used.

Note that Line 73-74 is in New York. Hence its outage results in a PV curve not much different from the base case PV curve. Lines 3-2 and 3-18 are near the buses with load increases, and thus the PV curves resulting from their outage show less stability margins. Lines 8-73 and 2-37 are interface lines between New York and New England. Their outages have significant impact on the voltage stability margin because part of the load increase in New England is supplied by a New York generator. From Table V, the contingency-based voltage stability margin is 944 MW for the load on Bus 16.

Table V
CONTINGENCY LIST FOR 48-MACHINE SYSTEM

Contingency	Line Outage	Pre-contingency Power Flow	Voltage Stability Margin
A	73-74	72 MW	1,346 MW
B	8-73	97 MW	944 MW
C	2-37	53 MW	1,221 MW
D	3-2	295 MW	1,005 MW
E	3-18	50 MW	1,231 MW

V. CONCLUSIONS

In this paper, we have developed a general-purpose power flow method that directly eliminates the matrix singularity issues that arise in PV curve calculations by introducing a new

AQ -bus type. The elimination of the singularity using the AQ -bus method was motivated using a classical two-bus system, and a framework was developed to include multiple load buses and multiple generators in the computation of PV curves. We presented two algorithms for practical implementation of the method and demonstrated both algorithms on a small two-area system. Finally, we extended the method to a 48-machine system to show its scalability and applicability to steady-state voltage stability margin calculation and contingency analysis.

This new method provides many advantages in the computation of steady-state voltage stability margins because it does not have numerical issues at the maximum power transfer point. Thus, power system operators can calculate the stability margins using this method far more reliably and quickly than a conventional power flow method.

ACKNOWLEDGMENT

This work was supported in part by the DOE/CERTS award 7040520 and in part by the Engineering Research Center Program of the National Science Foundation and the Department of Energy under NSF Award Number EEC-1041877 and the CURENT Industry Partnership Program. We like to thank DOE project managers Dejan Sobajic, Joe Eto, and Phil Overholt for their support.

REFERENCES

- [1] A. Kurita and T. Sakurai, "The power system failure on July 23, 1987 in Tokyo," in *Proc. of the 27th Conf. on Decision and Control*, 1988.
- [2] F. Bourgin, G. Testud, B. Heilbronn, and J. Verseille, "Present Practices and Trends on the French Power System to Prevent Voltage Collapse," *IEEE Transactions on Power Systems*, vol. 8, no. 3, pp. 778–788, 1993.
- [3] G. Andersson, P. Donalek, R. Farmer, N. Hatziargyriou, I. Kamwa, P. Kundur, N. Martins, J. Paserba, P. Pourbeik, J. Sanchez-Gasca, R. Schulz, A. Stankovic, C. Taylor, and V. Vittal, "Causes of the 2003 major grid blackouts in North America and Europe, and recommended means to improve system dynamic performance," *IEEE Transactions on Power Apparatus and Systems*, vol. 20, no. 4, pp. 1922–1928, November 2005.
- [4] C. Taylor, *Power System Voltage Stability*. New York: McGraw-Hill, 1994.
- [5] T. Van Cutsem and C. Vournas, *Voltage Stability of Electric Power Systems*. New York: Springer Science+Business Media, 1998.
- [6] K. Iba, H. Suzuki, M. Egawa, and T. Watanabe, "Calculation of critical loading condition with nose curve using homotopy continuation method," *IEEE Transactions on Power Systems*, vol. 6, no. 2, pp. 584–593, 1991.
- [7] V. Ajjarapu, *Computational Techniques for Voltage Stability Assessment and Control*. New York: Springer Science+Business Media, 2006.
- [8] H.-D. Chiang, A. Flueck, K. Shah, and N. Balu, "CPFLOW: a practical tool for tracing power system steady-state stationary behavior due to load and generation variations," *IEEE Transactions on Power Systems*, vol. 10, no. 2, pp. 623–634, 1995.
- [9] Y. Guo, B. Zhang, W. Wu, Q. Guo, and H. Sun, "Solvability and Solutions for Bus-Type Extended Load Flow," *Electrical Power and Energy Systems*, vol. 51, pp. 89–97, 2013.
- [10] B. Stott, "Review of load-flow calculation methods," *Proceedings of the IEEE*, vol. 62, no. 7, pp. 916–929, 1974.
- [11] M. Klein, G.J. Rogers, and P. Kundur, "A fundamental study of inter-area oscillations in power systems," *IEEE Transactions on Power Systems*, vol. 6, pp. 914–921, Aug. 1991.
- [12] J. H. Chow, R. Galarza, P. Accari, and W. Price, "Inertial and slow coherency aggregation algorithms for power system dynamic model reduction," *IEEE Trans. on Power Systems*, vol. 10, no. 2, pp. 680–685, 1995.

Scott G. Ghiocel (S'08) is a postdoctoral research fellow at the Center for Future Energy Systems at Rensselaer Polytechnic Institute. He received his PhD degree in Electrical Engineering from RPI in 2013. His research interests include power system dynamics, voltage stability, and applications of synchronized phasor measurements.

Joe H. Chow (F'92) received his BS degrees in Electrical Engineering and Mathematics from the University of Minnesota, Minneapolis, and MS and PhD degrees, both in Electrical Engineering, from the University of Illinois, Urbana-Champaign. After working in the General Electric power system business in Schenectady, New York, he joined Rensselaer Polytechnic Institute in 1987, and is a professor of Electrical, Computer, and Systems Engineering. His research interests include multivariable control, power system dynamics and control, voltage-source converter-based FACTS controllers, and synchronized phasor data.

Chapter 3: Thevenin Equivalent Calculation

The details of the method for computing Thevenin equivalents are contained in the paper

S. G. Ghiocel, J. H. Chow, G. Stefopoulos, B. Fardanesh, D. Maragal, D. B. Bertagnolli, M. Swider, M. Razanousky, D. J. Sobajic, and J. H. Eto, "Phasor-Measurement-Based Voltage Stability Margin Calculation for a Power Transfer Interface with Multiple Injections and Transfer Paths," *Proceedings of Power System Computation Conference*, Wroclaw, Poland, 2014.

The paper is attached below.

PHASOR-MEASUREMENT-BASED VOLTAGE STABILITY MARGIN CALCULATION FOR A POWER TRANSFER INTERFACE WITH MULTIPLE INJECTIONS AND TRANSFER PATHS

Scott G. Ghiocel, Joe H. Chow
Rensselaer Polytechnic Institute
Troy, New York, USA
ghiocel@alum.rpi.edu, chowj@rpi.edu

David B. Bertagnolli
ISO-New England
Holyoke, Massachusetts, USA
dbertagnolli@iso-ne.com

Michael Razanousky
New York State Energy Research and
Development Authority (NYSERDA)
Albany, New York, USA
mpr@nyserd.org

George Stefopoulos, Bruce Fardanesh,
Deepak Maragal
New York Power Authority
White Plains, New York, USA
George.Stefopoulos@nypa.gov, Bruce.Fardanesh@nypa.gov,
Deepak.Maragal@nypa.gov

Michael Swider
New York Independent System Operator
Rensselaer, New York, USA
MSwider@nyiso.com

Dejan J. Sobajic
Grid Consulting LLC
San Jose, California, USA
dsobajic@gridengineering.com

Abstract - For complex power transfer interfaces or load areas with multiple in-feeds, we present a method for phasor-measurement-based calculation of voltage stability margins. In the case of complex transfer paths with multiple injections, a radial system approach may not be sufficient for voltage stability analysis. Our approach provides voltage stability margins considering the full fidelity of the transfer paths.

In this paper, we extend a previously proposed phasor-measurement-based approach [1] and apply it to a voltage stability-limited power transfer interface using synchronized phasor measurements from loss-of-generation disturbance events. Previous work employed a simple radial system [2] or modeled a power transfer interface using only one generator [1]. In our approach, we use the PMU data to model multiple external injections that share the power transfer increase, and we employ a modified AQ -bus power flow method to compute the steady-state voltage stability margins [3]. We demonstrate the method using real PMU data from disturbance events in the US Eastern Interconnection.

Keywords - voltage stability, phasor measurements, stability margins

1 Introduction

THIS paper is primarily concerned with the use of phasor measurement unit (PMU) data for voltage stability margin calculation. Because of the increasing number of PMU installations, applications of synchrophasor data for voltage stability are of interest to system operators to mitigate the risk of major blackouts [4, 5, 6]. Loss-of-generation events can cause voltage collapse and cascading failures by depleting the reactive power in critical areas, overloading transmission lines, and/or causing sudden power transfer shifts. For these events, we can observe the dynamic behavior of the system power flows and voltages using high-sampling rate phasor measurements. The

power flow and voltage sensitivities from the phasor measurement data can provide valuable information regarding the system condition.

Voltage stability analysis typically requires significant computation which hinders real-time applications. One approach is to reduce the system to a radial network, from which the maximum loadability can be readily computed [7]. This idea has been applied in previous work [2] for radial-type transfer paths. However, a complex transfer path with multiple injections cannot always be reduced to a radial network. In other cases, a load area can have multiple in-feeds that increase the complexity of the voltage stability analysis. Previously in [1], we analyzed part of a meshed transfer path using PMU data from one substation, but the lack of PMU coverage limited our analysis to one Thévenin equivalent generator to represent the increased power transfer. In that work, we did not compute the PV curve to the maximum loading condition due to the ill-conditioned Jacobian matrix of the power flow solution.

In this paper, we have better PMU coverage of the same transfer interface with six PMUs at multiple substations, and we construct Thévenin equivalents for all of the external injections of the transfer path to maintain the full fidelity of the transfer path. We extract voltage variations from the phasor measurement data to construct Thévenin equivalents and quasi-steady-state models for the external injections, including FACTS controllers such as SVCs and STATCOMs. Selected PMU data points are used to estimate the parameters of the external injection models. Finally, we use a newly developed AQ -bus power flow method to compute the steady-state voltage stability margins quickly and efficiently [3]. Our approach is demonstrated using PMU data from loss-of-generation events on the Central New York power system. The PMU data for

one such event is shown in Fig. 1, where we plot the variation of the bus voltage magnitude versus interface power transfer (PV curve).

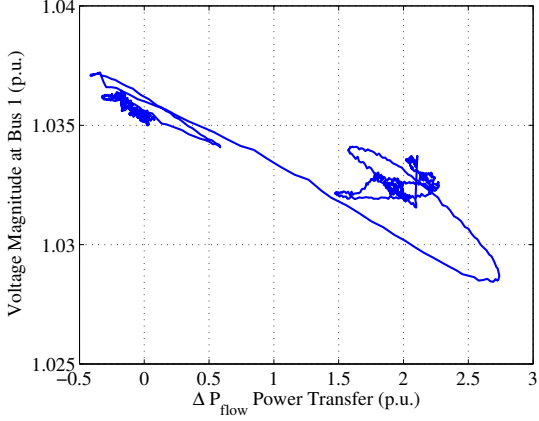


Figure 1: PV plot using PMU data for a loss-of-generation event.

The rest of the paper is organized as follows. In Section 2, we discuss the Central New York power system and disturbance events. In Section 3, we present the external injection models and the calculation of their parameters. In Section 4, we extrapolate the voltage stability margins using the computed external injection models, and we conclude in Section 5.

2 Central NY Power Transfer Path

The first stage in our analysis is use a phasor-measurement-based state estimator to correct errors and compute unmeasured quantities in the observable portion of the network [8]. The observable network including the transfer path is shown in Fig. 2, and external injections are shown as arrows into or out of the network. The transfer path of interest consists of Lines 1–2 and 1–3, where power generally flows from left to right from Bus 8 to the external system beyond Bus 2.

The transfer path will show an increase in flow toward Bus 2 after a loss-of-generation event occurs in the external system. Because there are other paths to the external system, the transfer path will only supply a portion of the lost generation. We study two such disturbances, which occurred during different system operating conditions. The events are listed in Table 1, along with the amount of lost generation and the post-contingency increase in power flow along the transfer path.

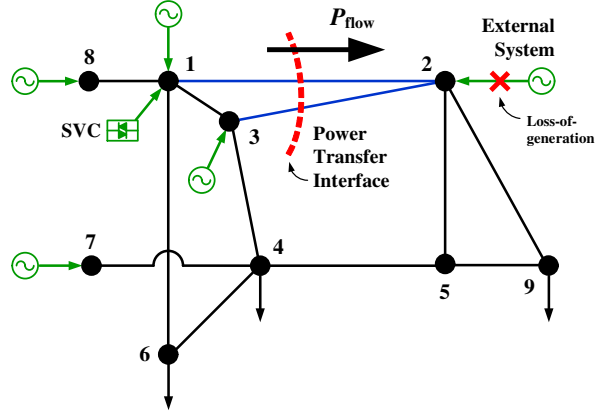


Figure 2: Central NY transfer path model.

Name	External gen. loss	ΔP_{flow}
Event 1	800 MW	300 MW
Event 2	700 MW	250 MW

Table 1: Loss-of-generation events in the external system and post-contingency interface flows.

In both cases, the increased power transfer is supplied by multiple generators. Unlike our previous work [1], we treat each generator separately using better PMU data coverage and a robust voltage stability solution method.

3 External Injection Models

3.1 Thévenin Equivalent Injection Model

The extent of the phasor-observable network is determined by the available phasor measurements [9], and the external portions of the system are unobservable. To build a model for voltage stability analysis, we model the external injections on the boundaries of the observable network using their quasi-steady-state equivalents. We retain the full fidelity of the phasor-observable network because it is quite small and there is little benefit in reducing it.

In the case of the Central New York power system, we use a Thévenin equivalent generator model for the injections at Buses 1, 2, 3, 7, and 8. The SVC at Bus 1 performs fast voltage regulation, so it is governed by its quasi-steady-state droop characteristic. The injections at Buses 4, 6, and 9 are loads with little participation in the disturbance, so we model them as fixed PQ loads. As our next step, we use the PMU data to compute the parameters of these external injection models with a nonlinear least-squares formulation.

Each of the Thévenin equivalent injection models consists of a stiff voltage source behind a reactance, as shown in Fig. 3.1. The voltage and current phasor quantities at the injection bus provide the means to estimate the parameters of the Thévenin equivalent model. We choose the injection bus voltage angle to be the reference angle to simplify the calculation.

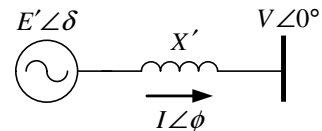


Figure 3: Thévenin Equivalent Generator Model

We use the phasor quantities to compute the Thévenin voltage E' and reactance X' using the equations

$$E' \cos \delta = V - X' I \sin \phi \quad (1)$$

$$E' \sin \delta = V + X' I \cos \phi \quad (2)$$

where δ is the machine angle, V is the voltage magnitude at the injection bus, and $I \angle \phi$ is the current injection phasor. Note that V and $I \angle \phi$ are either measured or computed using the state estimator, the unknown quantities E' and reactance X' are taken to be fixed values, and the unknown angle δ is allowed to vary between measurements. Thus we have 2 constant unknowns (E' , X') and for each measurement, we add 2 equations and 1 additional unknown (δ).

For a set of N measurements, we can formulate a non-linear least-squares estimation problem using (1) and (2), such that

$$\min_x f(x) = \left\| \begin{array}{c} E' \cos \delta_1 - V_1 + X' I_1 \sin \phi_1 \\ E' \sin \delta_1 - X' I_1 \cos \phi_1 \\ \vdots \\ E' \cos \delta_N - V_N + X' I_N \sin \phi_N \\ E' \sin \delta_N - X' I_N \cos \phi_N \end{array} \right\|_2 \quad (3)$$

where $x = [E' \ X' \ \delta_1 \ \dots \ \delta_N]^T$, and δ_k , V_k , I_k , and ϕ_k are the values corresponding to the k th data point. To solve the problem, we require at least as many equations as unknowns. In this case, there are $2N$ equations and $N + 2$ unknowns, so to satisfy the necessary condition we require at least two data points ($N \geq 2$). It should be noted, however, that the data points must represent at least two distinct operating points. Otherwise, there is not enough information to solve the least-squares problem.

Because we are assuming fixed voltage sources for the generators, we should avoid choosing data points during the period where the generator internal voltage can be varying, i.e., during the disturbance transients. In Fig. 3.1 we illustrate the selection of data points for computing the model parameters.

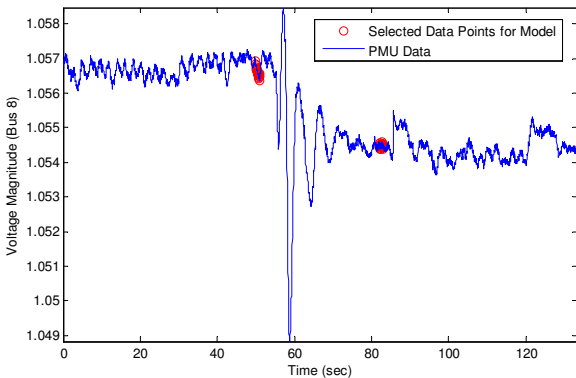


Figure 4: Selecting PMU data for Thévenin equivalent estimation.

Thus the selected data points (highlighted in red) are drawn from the pre-disturbance and post-disturbance mea-

surements, which represent two distinct operating points. For this study, the pre-disturbance data was not sufficient to calculate the Thévenin equivalent because it only covered one operating point. In practice, one can use additional pre-disturbance data covering multiple operating points to provide enough information to estimate the Thévenin equivalent parameters

3.2 SVC Injection Model

The SVC in at Bus 1 is typically operated in voltage control mode. Because of the fast time constants of the SVC compared the PMU sampling rate (and multiple-cycle averaging effects of the PMU), we assume the SVC is in a quasi-steady-state and follows its voltage regulation droop characteristic, given by

$$I_{SVC} = \frac{V - V_{ref}}{\alpha} \quad (4)$$

where I_{SVC} represents the magnitude of the current injection of the SVC into the network [10]. We use the phasor measurements of voltage and output current to estimate the voltage reference V_{ref} and droop α . In this frame of reference, the current leads the voltage by 90 degrees, so a negative value indicates reactive power injection by the SVC. We formulate the least-squares estimation as the optimization problem

$$\min_{V_{ref}, \alpha} f(V_{ref}, \alpha) = \left\| \begin{array}{c} (V_{ref} - V_1) - \alpha I_1 \\ \vdots \\ (V_{ref} - V_N) - \alpha I_N \end{array} \right\|_2 \quad (5)$$

where $I_k = I_{SVC}$ for the k th measurement and V_{ref} and α are assumed constant. Thus we have N equations and 2 unknowns, so at least two measurements are required.

4 Voltage Stability Margin Calculation

We use power flow calculations with the computed external injections model to generate PV -curves for the transfer path, increasing power transfer across the interface at every iteration. We compare these new PV -curves from the model to the original phasor measurement data to validate the model and examine the system behavior as the power transfer increases. We then use the computed PV curves to calculate the voltage stability margin using the maximum loading condition.

4.1 Estimation of injection model parameters

Using the method described in the Section 3, we first compute the Thévenin equivalent injection models. These injections are located at Buses 1, 2, 3, 7, and 8. The calculated parameters are given in Table 2.

Parameter	Event 1	Event 2
E'_1 (p.u.)	1.149	1.129
X'_1 (p.u.)	0.026	0.024
E'_2 (p.u.)	1.003	1.071
X'_2 (p.u.)	0.050	0.044
E'_3 (p.u.)	0.967	0.990
X'_3 (p.u.)	0.061	0.035
E'_7 (p.u.)	1.049	1.040
X'_7 (p.u.)	0.071	0.061
E'_8 (p.u.)	1.046	1.041
X'_8 (p.u.)	0.023	0.018

Table 2: Estimated Thévenin equivalent parameters

Most of the parameters are quite consistent between events. Because the Thévenin equivalent represents a group of generators, the status of remote generators can affect the values of the parameters.

The next step is estimating the SVC parameters V_{ref} and α using (5) with the PMU data from Events 1 and 2. The estimated parameters are given in Table 3.

Event	V_{ref} (p.u.)	α
1	1.037	0.0339
2	1.040	0.0325

Table 3: Estimated SVC parameters

We observe that the estimated parameters are consistent between the two events, which is expected because the SVC parameters are not changed frequently by the system operators. In Figures 5 and 6, we compare the estimated model to the PMU data and find a good match.

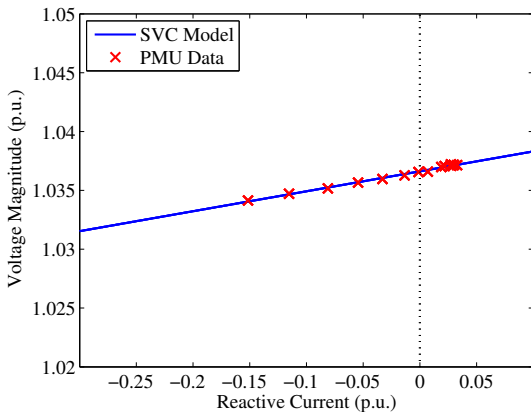


Figure 5: Comparison of SVC model to PMU data (Event 1)

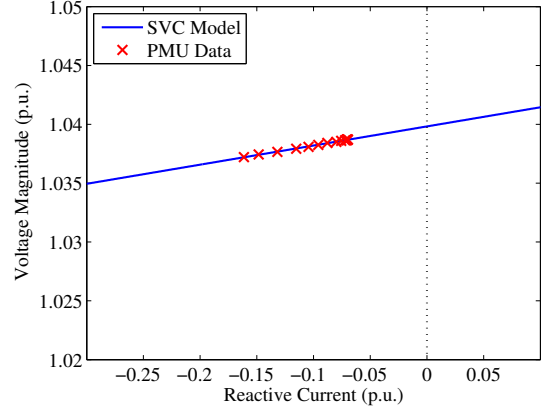


Figure 6: Comparison of SVC model to PMU data (Event 2)

After computing the parameters for all the injection models, we can establish a reduced model for voltage stability margin calculation.

4.2 PV curve computation using the AQ-bus method

The power flow is computed using a system model that includes the full detail of the transfer path, with the Thévenin equivalents at the external injection buses (Buses 1, 2, 3, 7, and 8) and the SVC model at Bus 1.

We use the AQ-bus power flow method [3] to compute the PV curves for the reduced model. The advantage of the AQ-bus method is that the Jacobian matrix singularity at the maximum loading condition is mitigated. In this approach, we choose an AQ bus and specify its voltage angle instead of active power. By increasing the angle separation between the swing bus and AQ bus, we indirectly increase the power flow to the AQ bus. Thus we run successive AQ power flows with increasing angle separation to compute the PV curve.

For the Central NY system, we choose Bus 2 as the AQ bus to represent increasing power transfer to the external system. The additional power transfer is supplied by the Thévenin equivalent generators connected to Buses 1, 3, 7, and 8, in proportion to their sensitivity to power transfer increases. These sensitivities (β) are readily computed from the PMU data as the ratio

$$\beta_i = \frac{\Delta P_i}{\Delta P_{\text{transfer}}} \quad (6)$$

where β_i is the sensitivity for the i -th generator, ΔP_i is the incremental power supplied by the i -th generator, and $\Delta P_{\text{transfer}}$ is the incremental power transfer across the interface. Using these sensitivities, we account for the fact that the generation loss is supplied by multiple generators over a meshed network.

Using data for each event, we compute PV curves for Buses 1 and 8 by increasing the angle separation between Bus 8 (swing bus) and Bus 2 (AQ bus). We include the SVC with its droop model and equipment limits.

4.3 Voltage stability margin calculation

In Figs. 7 and 8, we plot the PV curves for the system using PMU data from Events 1 and 2, respectively.

In these plots, the x -axis represents the incremental power flow across the interface and the y -axis represents the bus voltage magnitude. On the same axes, we plot the PMU data for comparison. From the plots, we can see that the model fits the data well. Note that the SVC reaches its equipment limits and saturates its output when the incremental power transfer reaches approximately 9 p.u., and the PV curve becomes slightly steeper at this point.

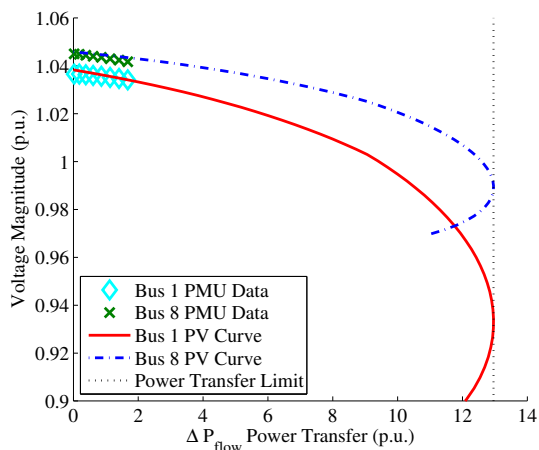


Figure 7: Comparison of computed PV curves to PMU data (Event 1)

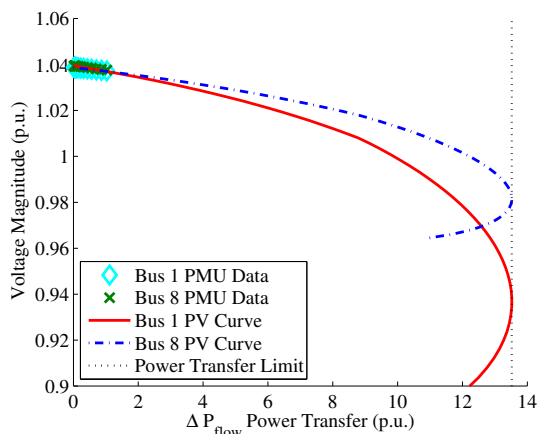


Figure 8: Comparison of computed PV curves to PMU data (Event 2)

In Fig. 9, we show a more detailed view of the overlapping PV curves for Event 2 and the corresponding PMU data.

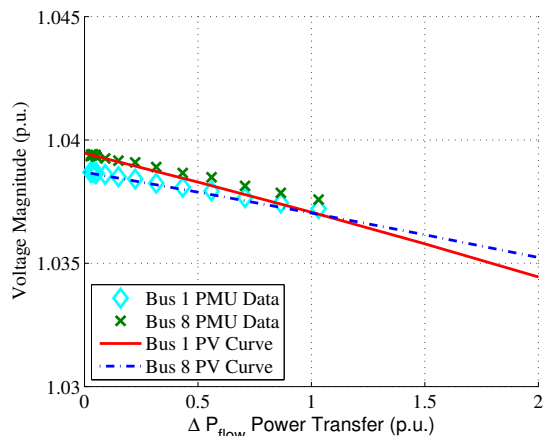


Figure 9: Close-up of PV curves for PMU Data (Event 2)

For each case, we calculate the stability margin by detecting and reporting the maximum value of the incremental power flow across the interface (ΔP) after the loss-of-generation event. The computed margins are summarized in Table 4.

Event	Gen. loss	ΔP_{flow}	Margin
1	800 MW	300 MW	1300 MW
2	700 MW	250 MW	1350 MW

Table 4: Post-contingency stability margins and incremental power transfer.

In both cases, the system was not heavily loaded so the stability margins are adequate. The results obtained agreed with transfer limits used in system operation.

5 Conclusions

In this paper, we presented a method for phasor measurement-based voltage stability analysis of a complex transfer path with multiple generation sources. We modeled the external system and power injections of the observable network using Thévenin equivalents. For an SVC in voltage control mode, we used the PMU data to calculate its voltage reference and droop characteristic, which corresponds to its quasi-steady-state operation. Using these models, we computed the PV curves and loadability margins using the AQ -bus power flow method and demonstrated agreement between the transfer path model and data.

As future work, we plan to extend the approach to larger systems with broader PMU coverage. We expect to conduct additional research on the applicability of the method to systems with more complex external injections, including renewable generation sources such as wind turbines. For these systems, one could use the approach described in this paper with different injection models.

Acknowledgement

The work described in this paper was coordinated by the Consortium for Electric Reliability Technology Solutions, and funded by the Office of Electricity Delivery and Energy Reliability, Transmission Reliability Program of the US Department of Energy (DOE) through a contract with Rensselaer Polytechnic Institute administered by the Lawrence Berkeley National Laboratory (LBL) via sub-contract 7040520 of prime contract DEAC03-05CH11231 between LBL and DOE. This research is also supported in part by the ERC Program of NSF and DOE under NSF Award EEC-1041877 and the CURENT Industry Partnership Program, and in part by NYSERDA Grant #28815.

References

- [1] S. Ghiocel, J. Chow, G. Stefopoulos, B. Fardanesh, D. Bertagnolli, and M. Swider, "A Voltage Sensitivity Study on a Power Transfer Path using Synchrophasor Data," in *IEEE Power and Energy Society General Meeting*, 2011, pp. 1–7.

- [2] M. Parniani, J. H. Chow, L. Vanfretti, B. Bhargava, and A. Salazar, "Voltage Stability Analysis of a Multiple-Infeed Load Center Using Phasor Measurement Data," in *IEEE PES Power Syst. Conf. and Exposition*, Atlanta, GA, Oct. 2006.
- [3] S. Ghiocel and J. Chow, "A Power Flow Method Using a New Bus Type for Computing Steady-State Voltage Stability Margins," *IEEE Transactions on Power Systems*, vol. 29, no. 2, pp. 958–965, Mar. 2014.
- [4] A. Kurita and T. Sakurai, "The Power System Failure on July 23, 1987 in Tokyo," in *Proc. of the 27th Conf. on Decision and Control*, 1988.
- [5] F. Bourgin, G. Testud, B. Heilbronn, and J. Verseille, "Present Practices and Trends on the French Power System to Prevent Voltage Collapse," *IEEE Transactions on Power Systems*, vol. 8, no. 3, pp. 778–788, 1993.
- [6] G. Andersson, P. Donalek, R. Farmer, N. Hatziaargyiou, I. Kamwa, P. Kundur, N. Martins, J. Paserba, P. Pourbeik, J. Sanchez-Gasca, R. Schulz, A. Stankovic, C. Taylor, and V. Vittal, "Causes of the 2003 Major Grid Blackouts in North America and Europe, and Recommended Means to Improve System Dynamic Performance," *IEEE Transactions on Power Apparatus and Systems*, vol. 20, no. 4, pp. 1922–1928, Nov. 2005.
- [7] D. Julian, R. Schulz, K. Vu, W. Quaintance, N. Bhatt, and D. Novosel, "Quantifying proximity to voltage collapse using the Voltage Instability Predictor (VIP)," in *IEEE Power Eng. Soc. Summer Meeting*, Seattle, WA, July 2000, pp. 931–936.
- [8] S. Ghiocel, J. Chow, G. Stefopoulos, B. Fardanesh, D. Maragal, B. Blanchard, M. Razanousky, and D. Bertagnolli, "Phasor-Measurement-Based State Estimation for Synchronphasor Data Quality Improvement and Power Transfer Interface Monitoring," *IEEE Transactions on Power Systems*, vol. 29, no. 2, pp. 881–888, Mar. 2014.
- [9] L. Vanfretti, J. H. Chow, S. Sarawgi, and B. Fardanesh, "A Phasor-Data-Based State Estimator Incorporating Phase Bias Correction," *IEEE Transactions on Power Systems*, vol. 26, no. 1, pp. 111–119, Feb. 2011.
- [10] N. Hingorani and L. Gyugyi, *Understanding FACTS: Concepts and Technology of Flexible AC Transmission Systems*. New York: Wiley-IEEE Press, 1999.

Chapter 4: BPA Wind Hub Voltage Stability Analysis

4.1 Develop network models for wind generation sites

One of the project accomplishments is to work with BPA to study the Jones Canyon wind turbine site (Figure 4.1) [4.1].

In this system, 6 wind farms are connected to the 230 kV Jones Canyon substation. The wind farms are all rated at about 100 MVA. Four wind farms are of Type 2 (induction generator) and the other two are of Type 3 (Doubly-Fed Asynchronous Generator, DFAG). The reactive power of the generators is supplemented by switched shunt capacitors of relatively small ratings. One of the Type-2 wind farm has a STATCOM rated at +/- 15 MVar. The (P,Q) flow output of each wind farm is measured. The statuses of the shunt capacitor banks are not known, and have to be estimated. The Jones Canyon substation is also equipped with two shunt capacitor banks with higher ratings.

The Jones Canyon substation is connected to the east via a relatively short line to the McNary 230 kV substation (East Bus), which is connected to the McNary 500 kV substation through a step-up transformer. The Jones Canyon substation is also connected to the west via a relatively long line to the Santiam substation (West Bus), which is connected to a 500 kV substation via a step-up transformer.

The intent of the study is to use a minimal set of measurements to enable the voltage stability analysis. The rationale is that if the measurements of the entire system is available, the problem would become a voltage stability analysis for the energy management system for the control center. Here the data requirements are:

1. Voltage and (P,Q) flow measurements of the individual wind farms and the East and West Buses. No measurements beyond the East and West Buses are used.
2. Line parameters of the network shown in Figure 4.1.

Because no measurements beyond the East and West Buses are used, it is assumed that they each are connected to a stiff bus via an impedance. Thus we have to develop a Thevenin equivalent at the West Bus, and one at the East Bus, as indicated in Figure 4.1. A least-squares procedure is used to estimate the Thevenin voltage at the stiff bus and the Thevenin impedance, as described in [4.2].

In the voltage stability analysis procedure in which the total output power of the wind farms is increased until a voltage collapse point is reached, the incremental wind power is divided 50-50 going to the East and West Buses.

In this setting, the AQ-bus method is applied to this wind hub system to determine the voltage stability limits for the wind farm outputs.

4.2 Perform voltage stability analysis

The objective of this investigation is to perform voltage stability analysis using the BPA wind hub network model and the Thevenin equivalents to compute the voltage stability margins for the wind hub.

It is important that the approach taken meets the expectation of the user. On June 2, 2014, the RPI project team (Joe Chow and Scott Ghiocel) met with BPA engineer Tony Faris, who is in Dr. Dmitry Kosterev's group. It was decided that for a demonstration of the approach, it would be applied to historical data, so that the results could be considered carefully before proceeding to a potential real-time application. The plan was for BPA to supply a week's worth of 24-hour data set containing all the required voltage and flow measurements at the wind hub system. As the PMU at Jones Canyon had not been installed yet, 2-sec SCADA data would be used. Furthermore, the voltage stability margin would be computed every 5 minutes, using the SCADA data for the last 5 minutes.

Thus computer code written in MATLAB was developed to perform these 5-minute VS calculation for the whole 24-hour record. The computation procedure is as follows:

1. For each 5 minutes, compute new Thevenin equivalents for the East and West Buses.
2. Increase the wind farm power output and use the AQ-bus method to compute the PV curves of at all three buses (which are computed simultaneously). The power margin is from the current operating condition to the point of voltage collapse.¹

The results of this set of 24-hour analysis are shown in Figures 4.2 to 4.7. These figures were generated by the graphical user interface. The 3 plots on the top left show the power delivered over time to the West Bus, the power generated by the wind hub, and the power delivered to the East Bus. The two plots in the middle left are the wind hub output power plotted against the maximum power output limit, and the voltage stability margin, that is, additional power that can be delivered by the wind hub. The three plots on the bottom left are the PV curves for the West Bus, the wind hub, and the East Bus. Note that the voltage at the wind hub is most sensitive to the power output. Note also that there are two curves in the PV curve plot: the red line is the short-term curve (that is, no capacitor switching) and the black line is the long-term curve (that is, shunt capacitors will switch when the voltage reaches a threshold).

Currently, a 24-hour analysis would require about 15-20 minutes of elapsed time on a laptop that is a couple of years old.

The right most column contains three plots. The top one is the measured voltages at the three buses. The lower two plots are the Thevenin voltages and impedances at the East and West buses.

Also note that no stability margin is computed if the output of the wind hub is zero. The assumption is that the wind turbines are off line.

¹ In some VS programs, voltage stability is defined by a low voltage threshold, which is not the same as the true collapse point voltage. This option can be applied here also.

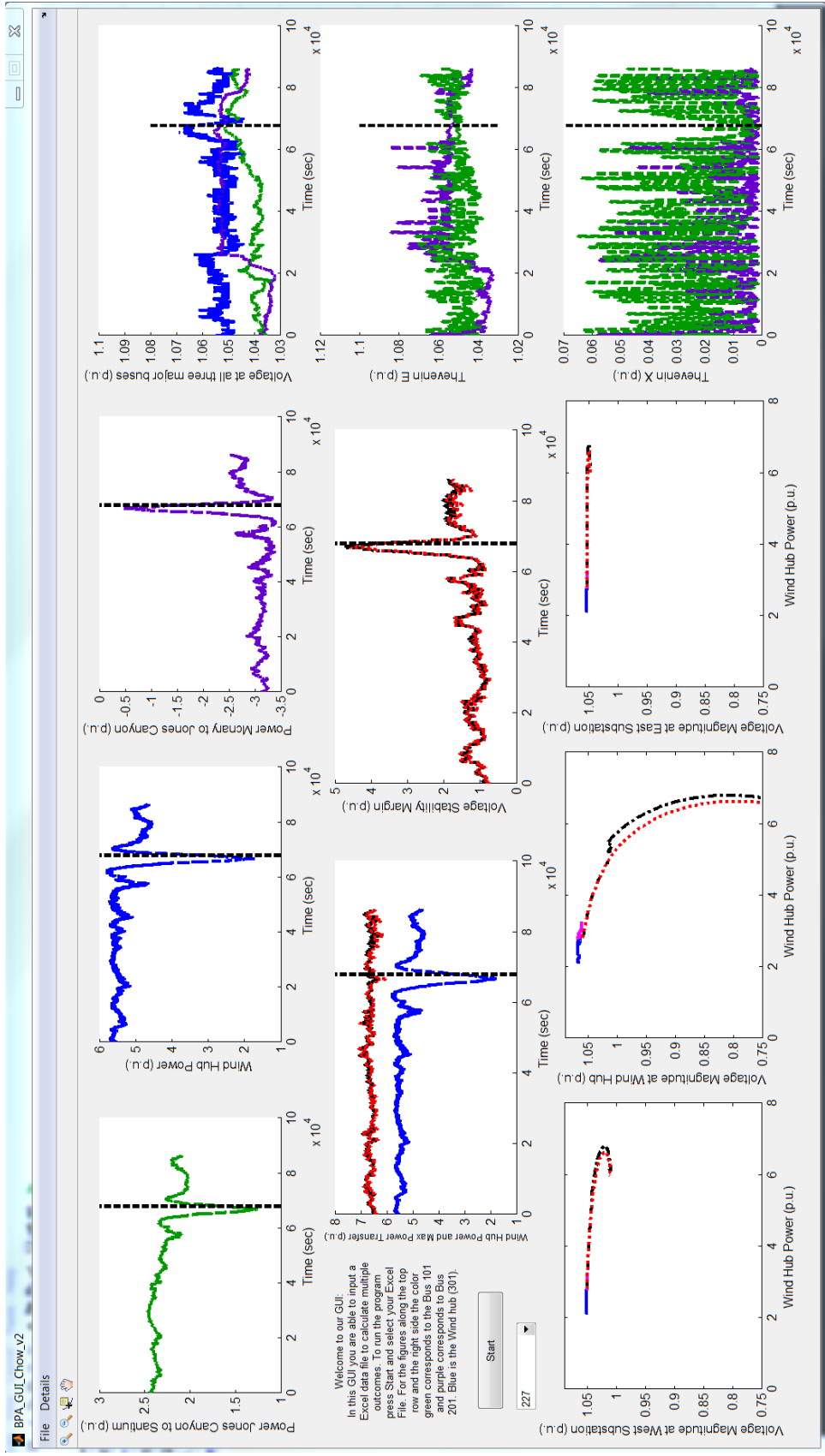


Figure 4.2. One-day voltage stability analysis for June 16, 2014

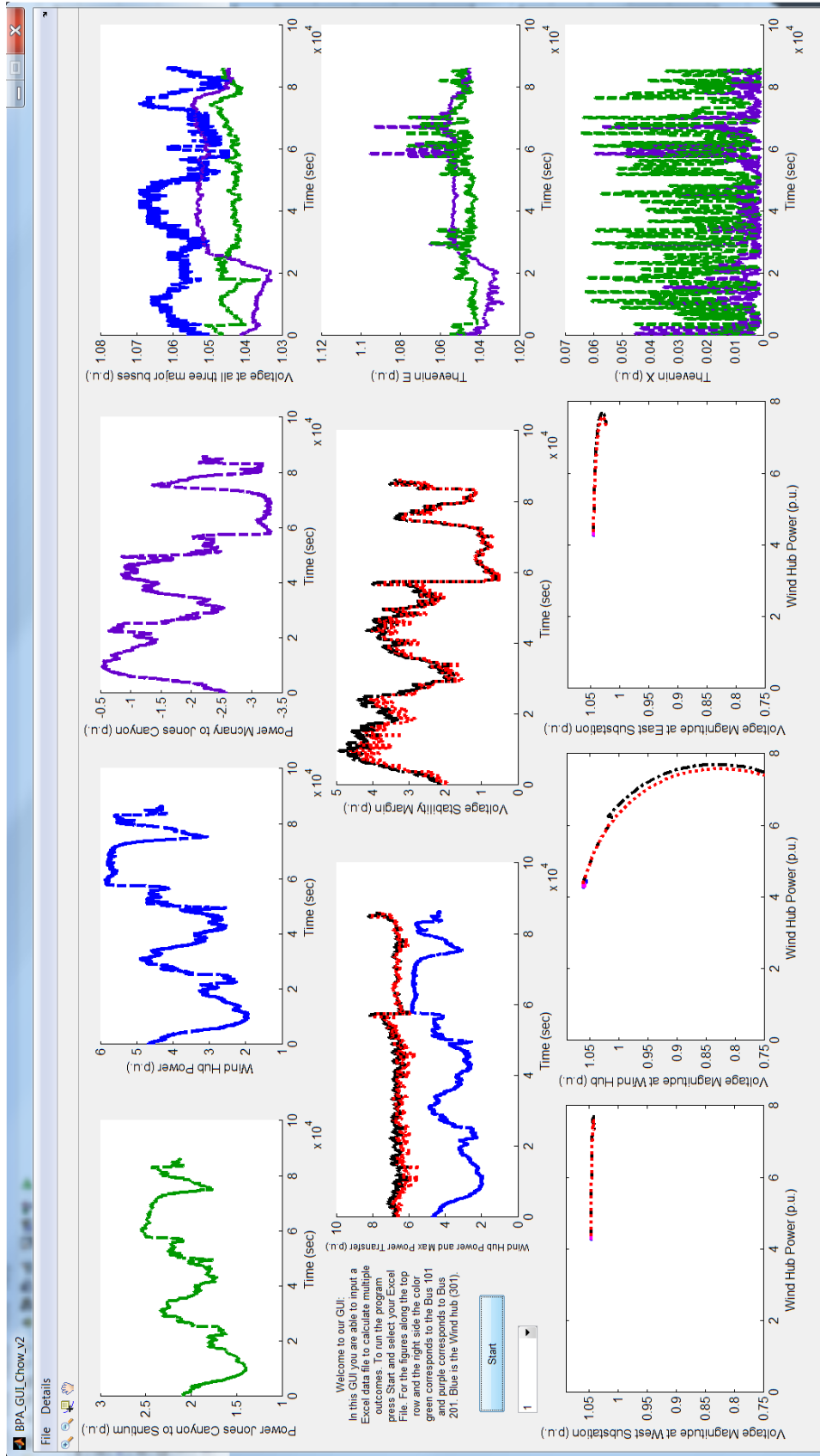


Figure 4.3. One-day voltage stability analysis for June 17, 2014

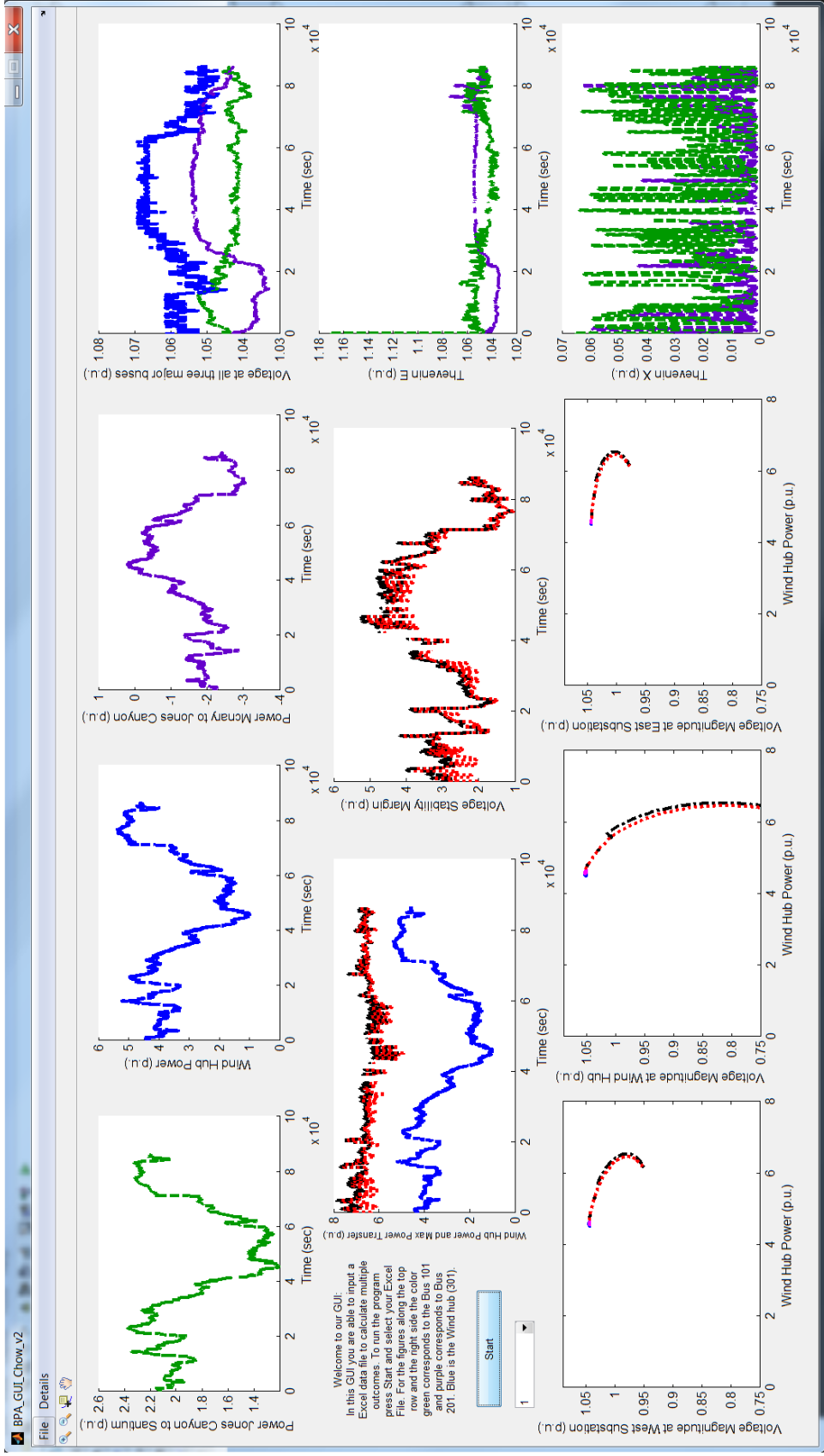


Figure 4.4. One-day voltage stability analysis for June 18, 2014

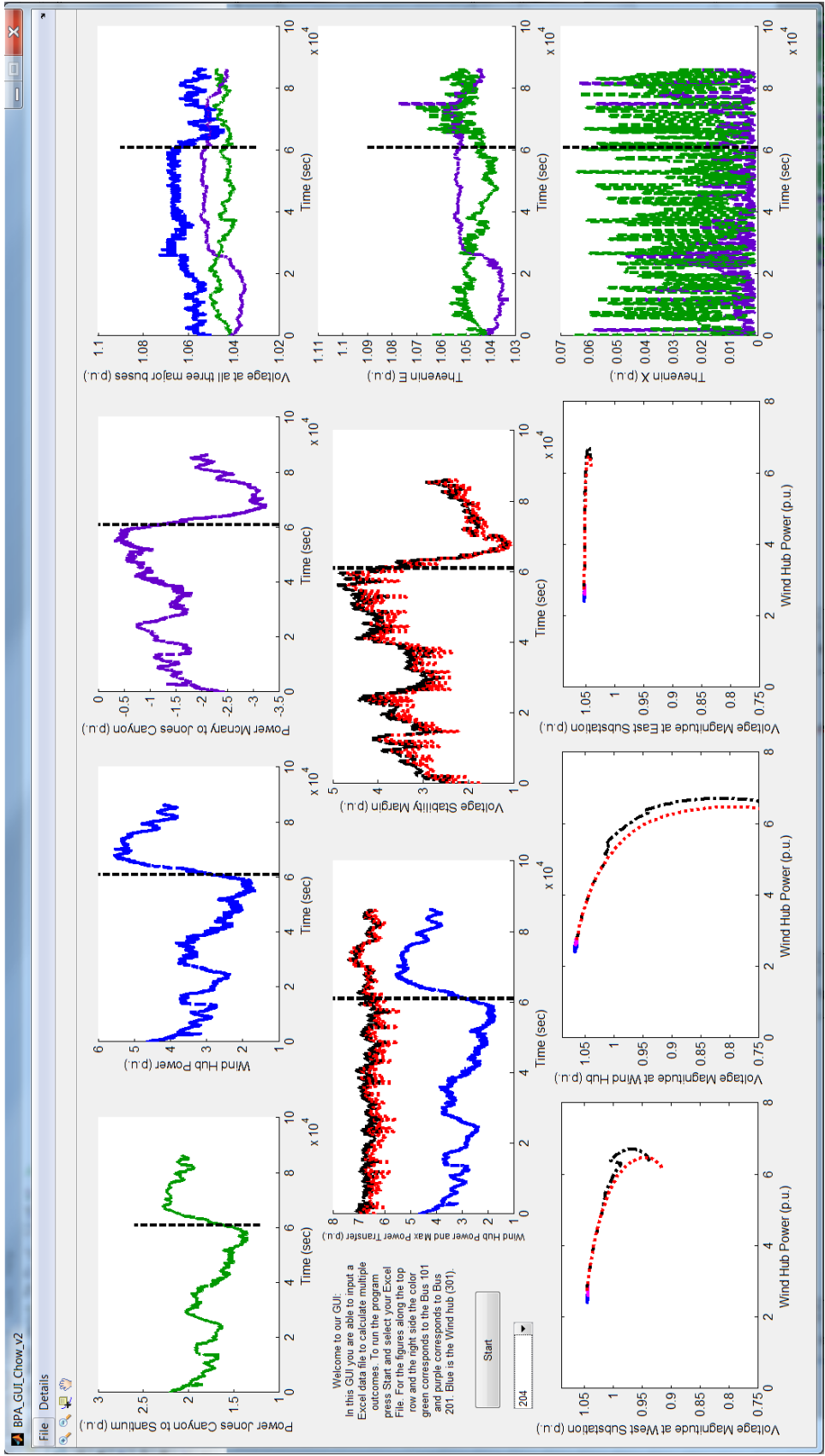


Figure 4.5. One-day voltage stability analysis for June 19, 2014

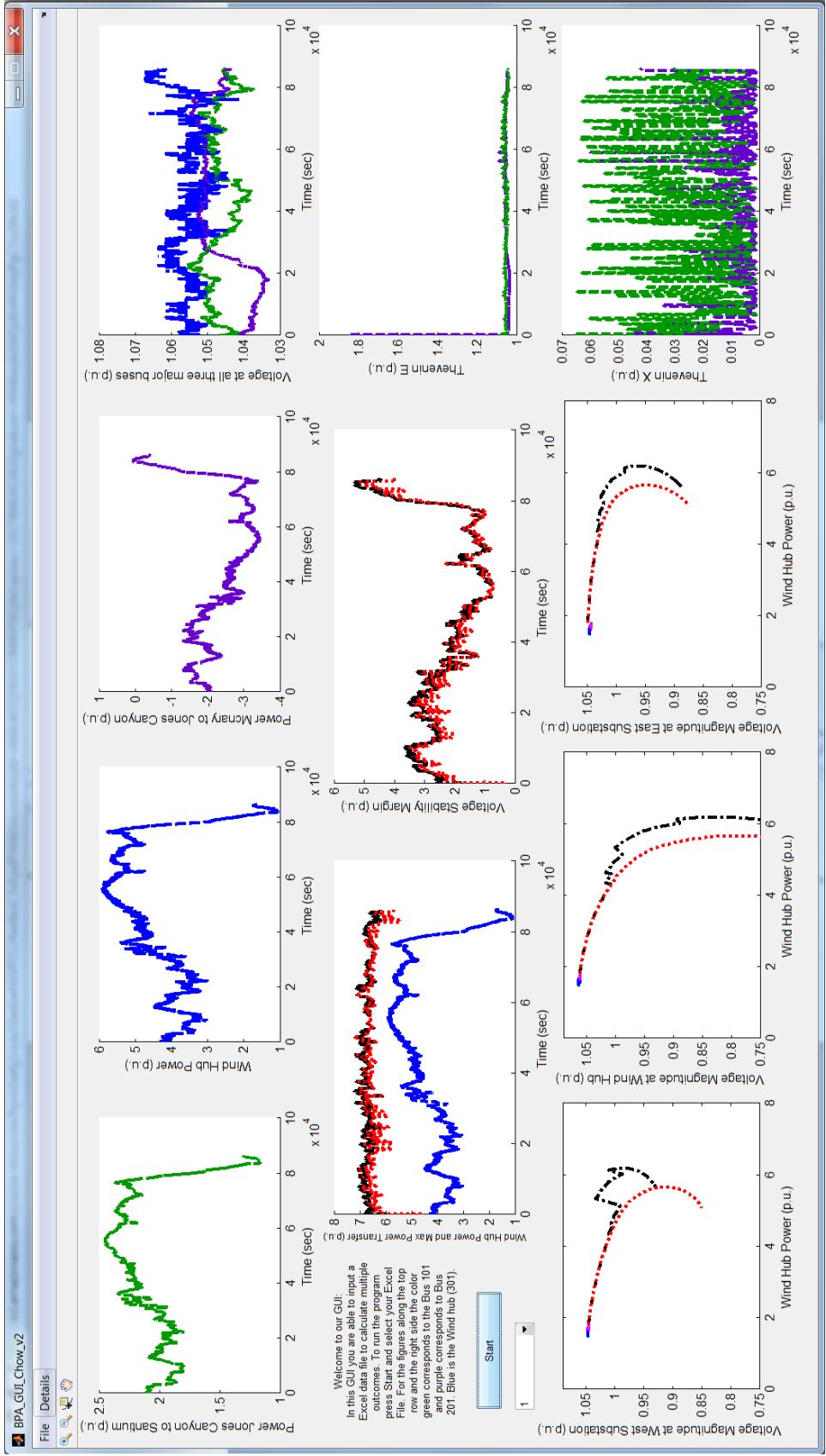


Figure 4.6. One-day voltage stability analysis for June 20, 2014

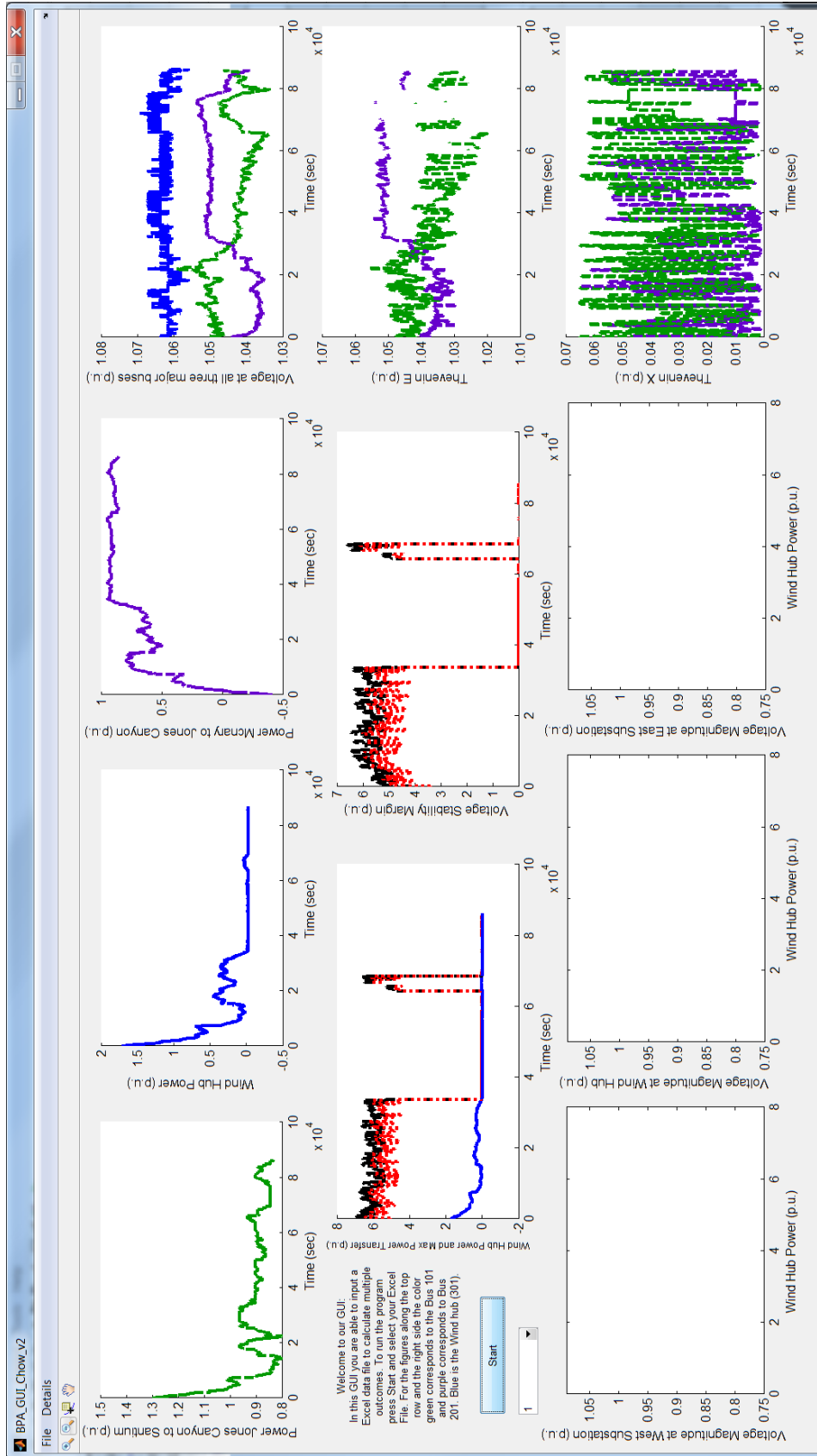


Figure 4.7. One-day voltage stability analysis for June 21, 2014

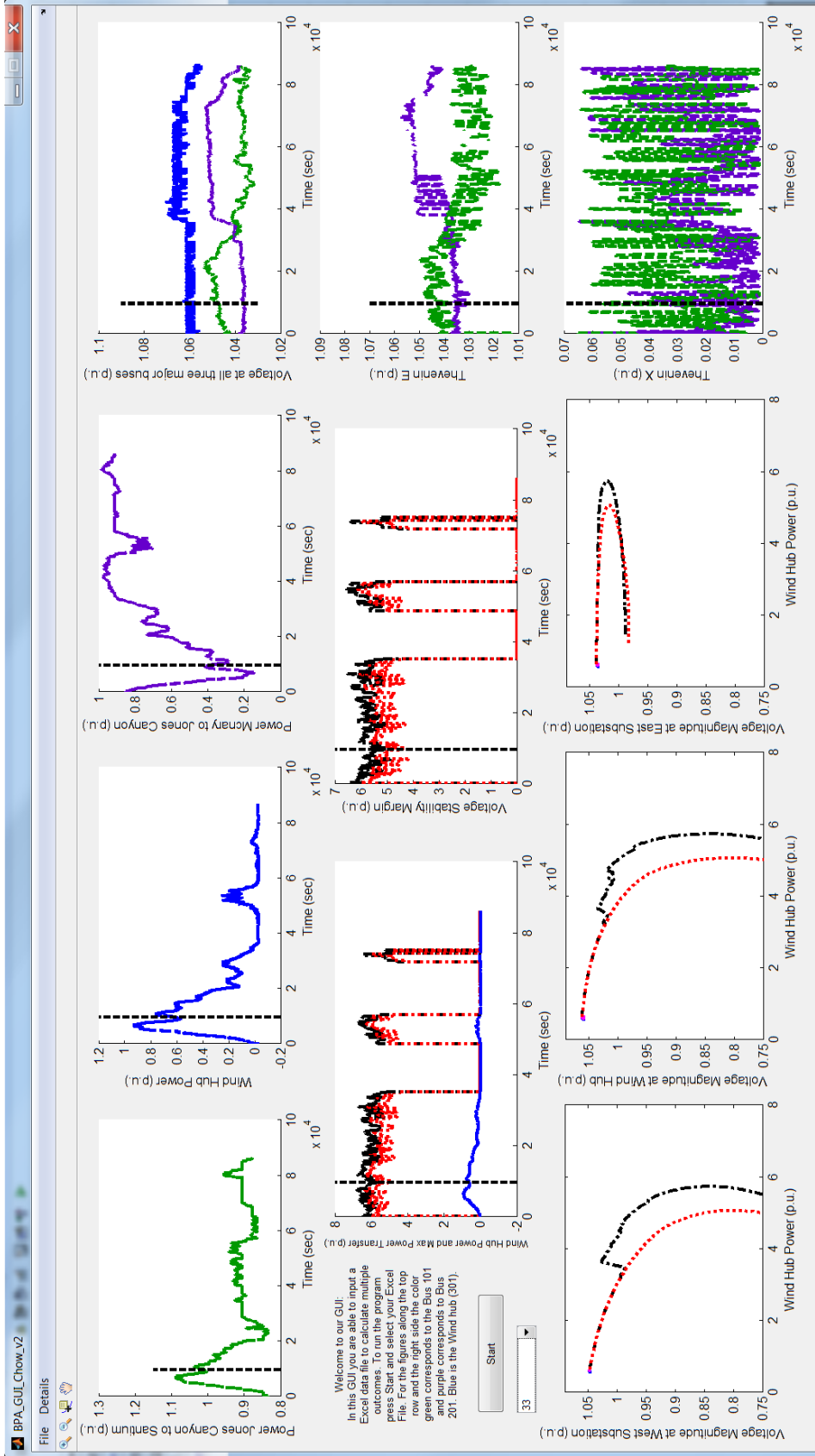


Figure 4.8. One-day voltage stability analysis for June 22, 2014

The VS analysis results seem to be quite reliable. The maximum power that can be delivered from the wind hub is about 650 MW, regardless of the loading condition on the two lines connecting to the East and West Buses.

The Thevenin equivalent voltage value tends to be quite steady, varying by one or two percent, but the Thevenin impedances tend to vary quite a bit. However, the impedance values are still quite a bit smaller than the impedances of the lines from the wind hub to the East Bus and the West Bus. The reasons for the time varying nature of the impedances are mostly due to:

1. Measurement noise, including quantization error in the wind hub voltage measurement
2. Steady voltage and power flow values that make it difficult to obtain sensitivities
3. Fast varying voltage and power flow values that induce nonlinear system behaviors, including wind turbine control systems and shunt capacitor bank switching.

Even though the Thevenin impedance value computed by the least-squares method shows significant variations, the analysis results still seem to be valid. In the future, it would be interesting to investigate more sophisticated algorithms such as the one proposed in [4.3].

We are in the process of preparing a paper to discuss the BPA wind hub investigation.

4.3 Real-time application strategies

One of the objectives of this project is to develop strategies for using the proposed voltage stability method in a real-time setting using PMU data collected by phasor data concentrator (PDC).

As mentioned earlier, the wind hub VS software (MATLAB code) will be provided to BPA for evaluation, which will be done on an off-line basis. The software has been applied to multiple days of the wind hub operation. Thus we expect the BPA engineer will be able to execute it without difficulties (like software crashes). We are committed to support the software during this evaluation phase, which may last beyond the completion date of the current project, as the graduate students who contributed to this effort are still studying for their PhD degrees.

Once the software has matured to the point that BPA would be interested to host it in real time, the following strategies can be considered:

1. Using streaming PMU data from the wind hub: In the BPA configuration, only data from Jones Canyon would be needed. Thus it would not require the use of a PDC, which collects PMU data from multiple substations. However, it is still convenient to host the real-time software on a PDC, as other similar types of wind hub operation may require additional PMU data other than the wind hub. In terms of the development effort, the VS software needs some input data streaming code.
2. Frequency of VS calculation: Currently the VS margin is calculated every 5 minutes. It is straightforward to change this time duration. The margin can be calculated more frequently, like every minute. The amount of data for the Thevenin equivalent calculation can also be varied. For example, although the margin is calculated every minute, the Thevenin equivalent can be based on the most recent 5-minute data (or longer). The process can even be made adaptive, allowing the algorithm to use as much data as needed to obtain a consistent set of Thevenin voltage and impedance.

3. System status: The accuracy of the method can be improved if the shunt capacitor statuses are provided, which will help in the computation of the Thevenin equivalent.
4. Wind turbine control systems: It is contemplated that the VS margin can be made more accurate if some information of the wind turbine active and reactive power control modules are available.

References

- [4.1] E. Heredia, D. Kosterev, and M. Donnelly, "Wind Hub Reactive Resource Coordination and Voltage Control Study by Sequence Power Flow," *2013 IEEE PES General Meeting*, July 2013.
- [4.2] S. G. Ghiocel, J. H. Chow, R. Quint, D. Kosterev, and D. J. Sobajic, "Computing Measurement-Based Voltage Stability Margins for a Wind Power Hub using the AQ-Bus Method," presented at the Power and Energy Conference at Illinois (PECI), 2014.
- [4.3] S. Corsi and G. N. Taranto, "A Real-Time Voltage Instability Identification Algorithm based on Local Phasor Measurements," *IEEE Transactions on Power Systems*, vol. 23, pp. 1271-1279, 2008.

Chapter 5: SCE Monolith Region Voltage Stability Analysis

5.1 SCE Wind Farm Study

The Tehachapi, California, is one of the best wind resource area in the country, as described by an NREL conference paper² published about 10 years ago. In this paper, the authors proposed several ways of providing reactive power support for the region, including a 45-MVar switched capacitors at 15 Mvar each installed at Monolith, and reactive power support at each wind farm.

Following the NREL study and based on system data provided by Armando Salazar of SCE, Figure 5.1 has been developed as a simplified electrical network connection of the Tehachapi wind region. In this system, 10 wind farms are connected to the 66 kV Antelope-Bailey system which Monolith substation is a part of. The wind farms can be separated into three groups; Windparks, Windlands, and Windfarms. Two windfarms Dutchwind and Flowind will also be included in this study. The total ratings for the windfarms are: Windparks (79.9 MW), Windfarms (144.5 MW), Windlands (73.5 MW), and the other two windfarms (54.5 MW). Thus the maximum output of the system is 352.4 MW/MVA. The total reactive power support given by shunt capacitors for the system is 180 MVar. The system base used in this study is 100 MVA.

The Monolith substation is directly connected to the three main groups of windfarms. Monolith is also connected to some smaller loads including the Cummings, Breeze, and Bor-Hav-Lor-Walker buses. The main load that is present in this area is the Windhub bus and will be considered the swing bus. It is also directly connected to every windfarm area.

² H. Romanowitz, E. Muljadi, C. P. Butterfield, and R. Yinger, "Var Support from Distributed Wind Energy Resources," Proceedings of World Renewable Energy Congress VIII, Denver, Colorado, 2004.

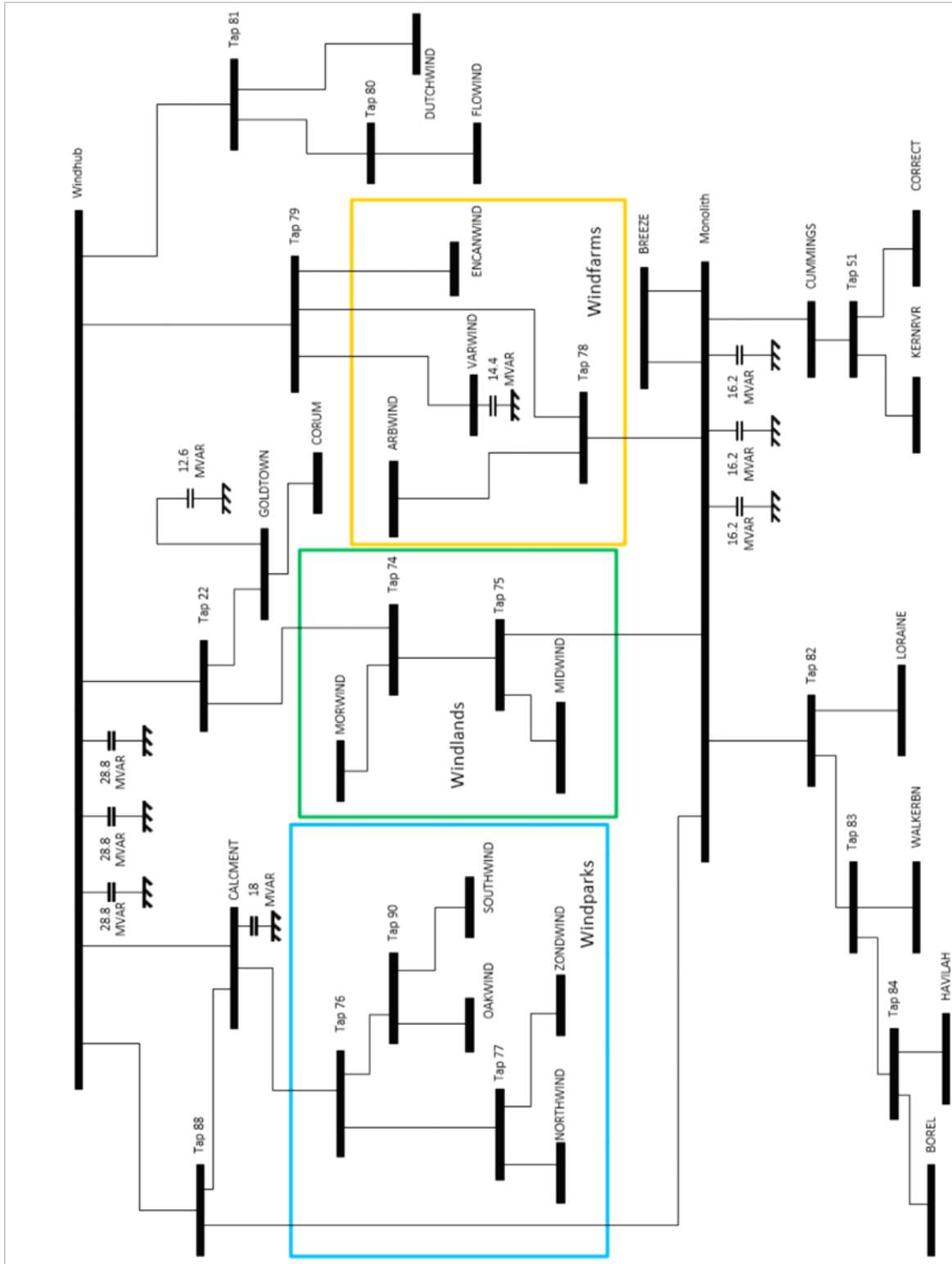


Figure 5.1: Monolith System Overview

This study will perform a voltage stability analysis for active power flowing from the windfarms to the areas of load. The maximum real and reactive power outputs and requirements will also be investigated. The data requirements for voltage stability analysis are:

1. Voltage and (P,Q) flow measurements of the individual wind farms and the Monolith and Windhub Buses. The measurements at the Monolith substation are down-sampled PMU data from the PMU located at Monolith. No measurements beyond the Windhub bus were used.
2. Line parameters of the network shown in Figure 5.1.

Because the main load that is present in this area is the Windhub bus, the largest amount of power will be flowing to this bus. In fact around 90% of the generation flows in this direction. The AQ-bus method is applied to the Windhub connection lines to determine the voltage stability limits for the wind farm outputs. The increase in power will be proportional to the maximum output of each windfarm.

5.2 Results

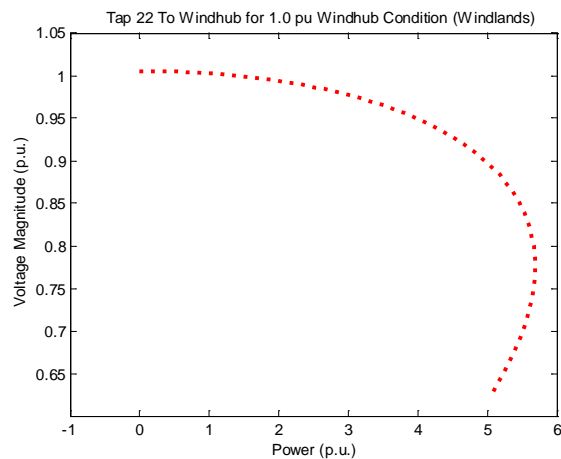
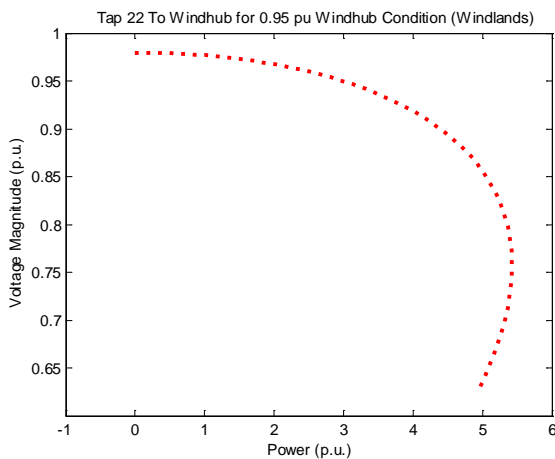
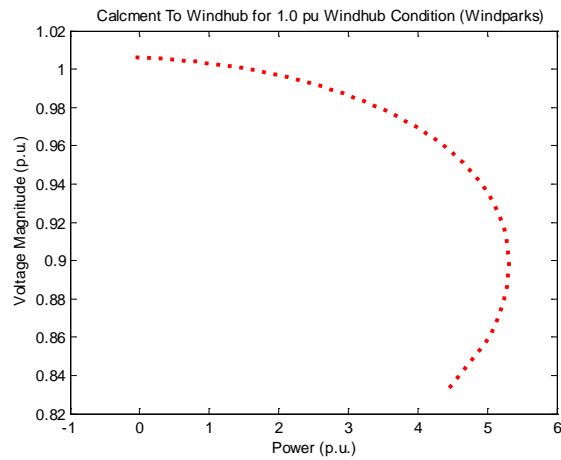
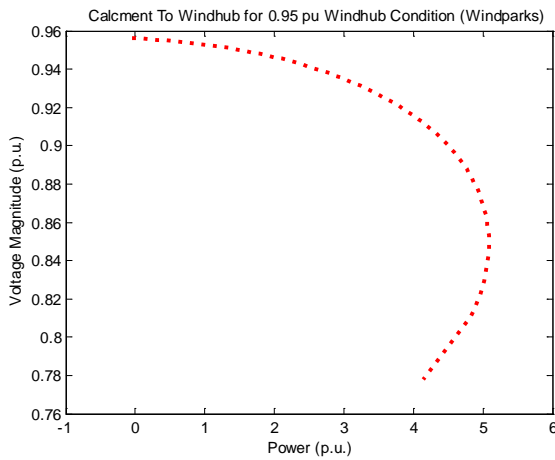
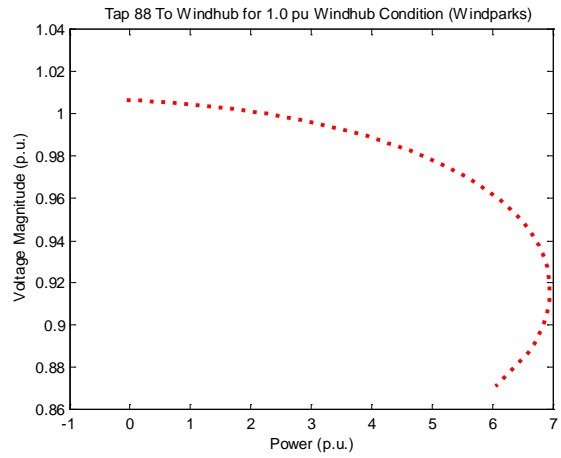
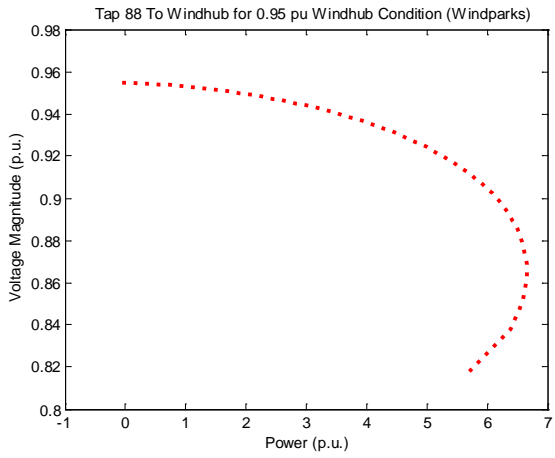
In order to utilize the AQ bus method we must push the power output out as far as possible. Thus, we will plot until and past the voltage collapse point. Two separate cases were performed for voltage stability analysis. Each case focused on the power flow through the lines directly connected to the Windhub bus. Case 1 represented a starting voltage of 0.95 pu for the Windhub bus whereas case 2 at a starting voltage of 1.0 pu for the Windhub bus. The results obtained from running the AQ bus method are plotted in Figure 5.2.

These results show a clear indication of voltage stability margins within the system. When looking at the maximum power output of the installed windfarms, of 3.524 pu, we see that the maximum power output will be reached well before the voltage collapse point. In fact, if the maximum output from the windfarms were to double, the system would still be considered within a stable region of operation. Furthermore, the most constraining paths are Tap 88, Cal Cement, and Tap 22, whereas Tap 79 and Tap 81 still have more transfer margin (as they have yet to show a voltage collapse point).

Using these plots, it seems that the system can handle more wind farms, in addition to those already installed. To illustrate, the PQ curve for the Windhub bus is plotted in Figure 5.3. This plot shows clearly the reactive power support needed to accommodate the increase in power generation.

Case 1: 0.95 pu Voltage at Windhub

Case 2: 1.0 pu Voltage at Windhub



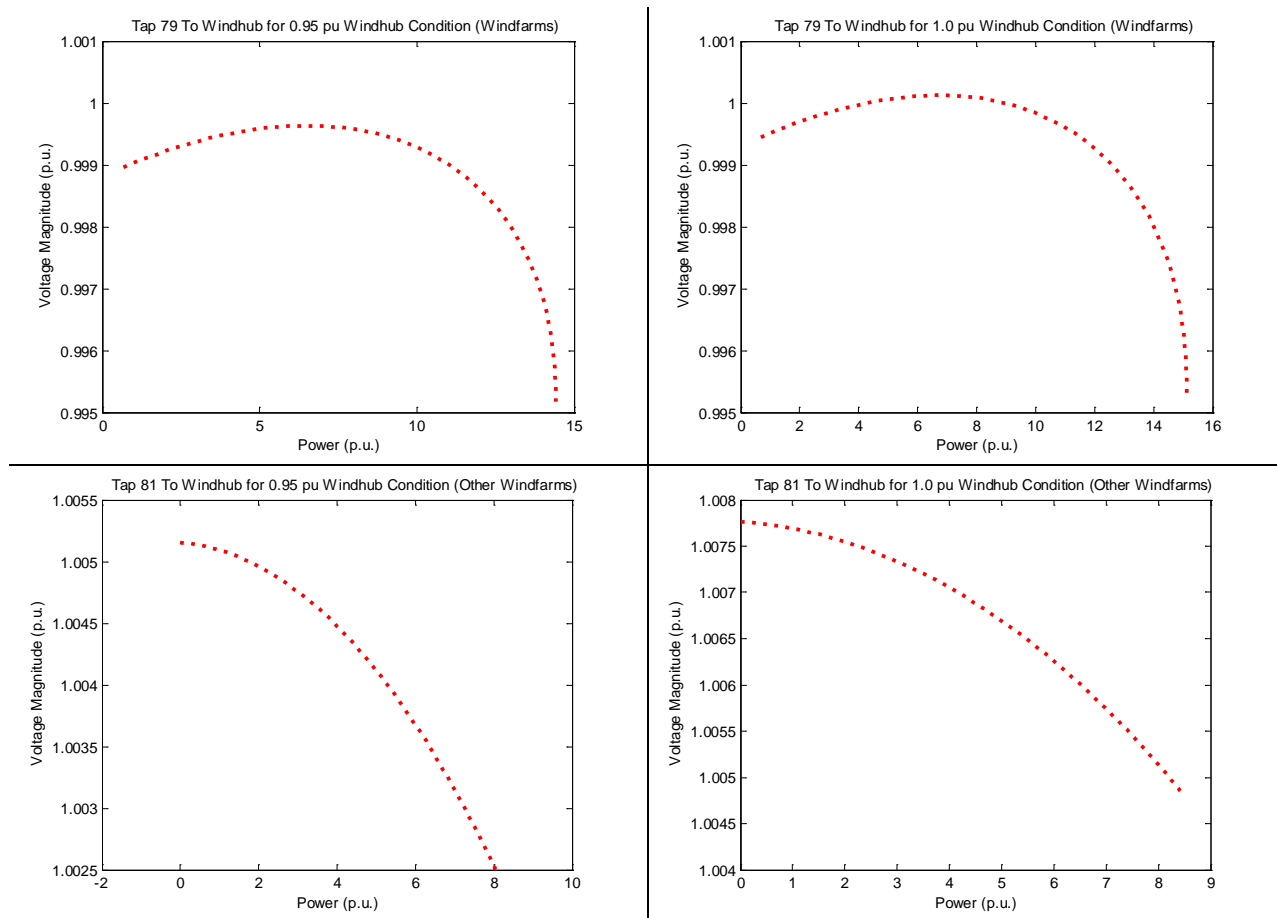


Figure 5.2: PV Curves for Power Transfer to Windhub Bus – left column: Windhub voltage starts at 0.95 pu, and right column: Windhub voltage starts at 1.0 pu

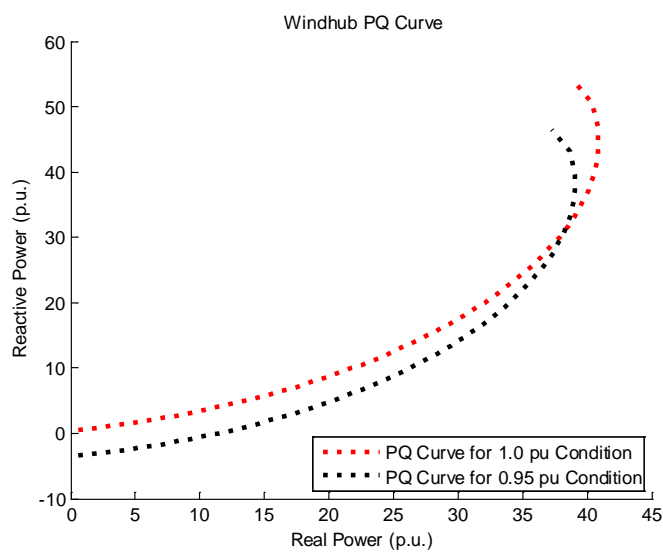


Figure 5.3: PQ Curves for Windhub Bus

Figure 5.3 shows that at higher levels of real power output, a large amount of reactive power is needed. At the current maximum power output the system’s reactive shunt support is clearly enough to handle the system. When the power is increased, some new shunt capacitors will need to be installed as well as the use of reactive power support from generators within the system. Some key values for the PQ curves are shown in Table 5.1.

Table 5.1: Values for Real and Reactive Power for 1.0 pu Condition

Real Power Flow	Reactive Power Flow Required
3.3514 pu	1.2183 pu
6.9009 pu	2.2743 pu
40.8775 pu	44.7453 pu

These values represent the reactive power support needed for real power flow through the combined lines to the Windhub bus. The first row represents the amount of flow for the current maximum generation of 3.524 pu (as the flow is around 90% of the generation). The second represents double the maximum and the third the maximum output of the PQ curve.

5.3 Conclusions

In this chapter we have shown the results of the AQ-bus method voltage stability analysis for the SCE Monolith system. At the current maximum real wind power output the system is voltage stable. The Monolith area can in fact hold a much larger amount of wind generation while maintaining stability. If the generation limit were to double through more wind farm installations, then the system would go beyond the shunt reactive power support. However, with more shunt installations (40 MVar) and increased use of reactive support from generators, the system should remain voltage stable. Further increase of wind farm installation would require substantial reactive power investment, or new transmission/distribution line investment.

Chapter 6: Technology Commercialization

6.1 Introduction

There are two major intellectual properties that have been developed in this project, namely, (1) the AQ-bus method for computing voltage stability margins, and (2) MATLAB code for computing the voltage stability margin for a wind hub.

6.2 AQ-bus method for computing voltage stability margins

The AQ-bus method is a simple but elegant means for computing voltage stability limits without encountering Jacobian matrix singularity at the critical voltage point. It eliminates the singularity by fixing the bus voltage angle at a critical load bus, thus reducing the size of the Jacobian matrix by 1. As such, it is much more efficient than the continuation power flow method.

This method was disclosed as an invention by RPI on March 22, 2013. Subsequently a patent application was filed by RPI on May 2, 2014, with a PCT number of US1437092.

Currently, RPI has an ongoing discussion with a commercial power system simulation software vendor for incorporating the AQ-bus method into its software.

6.3 MATLAB code for computing the voltage stability margin for a wind hub

The MATLAB code is currently being used by BPA for off-line computation of voltage stability margins at the Jones Canyon wind hub. This software contains two main components: the AQ-bus method and a Thevenin equivalent voltage and reactance estimation method. The code can be licensed as is. However, we are still working on additional methods for obtaining more consistent Thevenin equivalent voltage and reactance values from measured voltage and current data.

Chapter 7: Conclusions and Recommendations

This is a timely project on advancing the state-of-the-art in voltage stability analysis and for applications to renewable resources. There are several contributions and recommendations for future work, which are listed as below.

The first contribution is the development of the AQ-bus method which is an efficient method for computing quasi-steady voltage stability margins, with the capability of computing the power flow solution all the way to the critical voltage point. The method is as straightforward and efficient to use as a conventional power flow program. A patent for this invention has been filed, and there is interest from a commercial power system simulation software vendor to incorporate this method. Thus the recommendation is to develop this method in simulation software suitable for large power systems, and apply it to very large power systems.

The second contribution is the development of methods to compute the Thevenin equivalent voltage and impedance from both SCADA and PMU measurement data. The least-squares method works well if the changes in voltage and current at the boundary bus is sufficiently large. If the variation is small, the method is not reliable. Additional research needs to be performed to develop more reliable methods.

Voltage stability margins on two wind hubs have been analyzed. In the BPA wind hub, fast and reliable voltage stability margins, both short-term and long-term, have been computed. The results, using measured data, show that it would not be possible to add another wind farm of 100 MW or more without additional reactive power compensation. A computer tool has been provided to BPA for off-line analysis to gain experience of the proposed method. The SCE wind hub investigation is akin to a planning study. Our results show that there seems to be sufficient voltage stability margins to add more wind farms in the area. For future work, studies on voltage stability analysis of additional wind hubs are recommended.